Master thesis

Torsion in ZIP bridge system - Appendices

Final version

Evert van Vliet
21-1-2012

Contents

A. Literature research

Compressive membrane action (CMA)

Other master students have done detailed literature research about the theory of CMA. In this report their findings will be shortly summarized to give an overview of the theory.

Introduction

CMA is also called " arching action", a very old concept in structural engineering. There are two important conditions that must be met to activate CMA. Firstly, the horizontal translation has to be (partly) restrained. Secondly, the net tensile strain along a longitudinal fibre must be non-zero when there is no horizontal restraint.[1]

To give an idea of the development of the ideas about CMA an short, not complete, historical overview is presented.[2,3] In 'A guide to compressive membrane action in bridge deck slabs' a very nice overview is given when the reader is interested in a more detailed description.

1909 Turner wrote something about arching effects in slabs.
1921 Westergaard and Slater found out some strength enhancement in concrete floor.
1936 Gvodzev published a paper to rationalise CMA in the Soviet Union.
1955 Ockleston did some load test and found out that the strength was higher than expected.
1956 McDowell et. al. proposed a theory to predict relative great strength of constrained masonry walls.
1958 Ockleston found out that CMA was the reason for the strength enhancement.
1960 Kinnunen and Nylander developed a model for punching capacity of unrestrained simply supported slabs.
1961 Wood tries to find a theory for CMA.
1964 Park tries to find a theory for CMA.
1975 Hewitt and Batchelor developed a theoretical approach for the estimation of the punching capacity of laterally restrained slabs by modifying the model of Kinnunen and Nylander.
1979 The Ontario Bridge Design Code utilized CMA as one of the earliest codes.
1980 Park summarized his theory in a book (Park and Gamble). Braestup provided a historical review of the analyses that have been developed. Most models assumed rigid-plastic concrete behaviour and rigid translation restrained. Therefore practical application was limited.
1985 Kirkpartic et. al. has done some experimental and analytical investigation of the punching capacity of the M-beam (commonlu used in UK). They found excessive capacity compared with the British design code. An empirical method was developed. That model wasn't able to handle varying degrees of restrained.
1992 Kuang and Moley investigated influence of the degree of edge restraint, percentage of steel reinforcement and span-depth ratio on the punching shear of columns supported by columns. The strength enhancement was thought to be due to CMA.
1993 Kuang and Moley presented a plasticity model that analyzes the effect of CMA.
1997 Rankin and Long presented a simple method predicting the enhanced ultimate flexural capacity of laterally-restrained slab strips. The loads carried by bending and CMA were considered separately and then added to give the total resistance. They used McDowell et. al.'s derivation.

[1] Bakker, G.J. (2008), *A finite element model for the deck of plate-girder bridges including compressive membrane action, which predicts the ultimate collapse load*, page 6.
[2] Han-Ug Bae (2008), *Design of reinforcement-free bridge decks with wide flange prestressed precast girders,* page 5.
[3] Taylor, dr. S. et.al. (2002), *Guide to compressive Membrane Action*

1998 Mufti and Newhook adapted the model proposed by Hewitt and Batchelor for punching capacity of a fibre reinforced deck.
2001 Taylor et. al. applied the theory of Rankin and Long (1997) to high-strength concrete slabs.
2003 Ruddle et. al. applied the method of Rankin and Long (1997) to Tee beams.
2003 Taylor et. al. proposed a procedure to evaluate the ultimate capacity of bridge deck slabs. The flexural capacity was calculated following the method of Rankin and Long and the punching shear by the method proposed by Kirkpatric et. al. The smallest capacity is the ultimate bearing capacity. This method doesn't include serviceability evaluation.

It's clear that for a long time a lot of research have been done. Also this is not all the research that is been done but a relevant selection for Han-Ug Bae. CMA is nowadays incorporated in the codes of New Zealand, Australia, Canada and the United Kingdom. This gives a good reason to continue research in Europe, especially in the Netherlands, to have also the advantageous effects.

In the next paragraphs a brief description of the basic theories and some interesting conclusions of other master students shall be given. For detailed description of the theory it will be better to read the report of De Rooij, that was the basis for this summary.

The studied reports about CMA are the following:

- Han-Ug Bae (2008), *Design of reinforcement-free bridge decks with wide flange prestressed precast girders*
- Wei, Xuying (2008), *Assesment of real loading capacity of concrete slabs*
- Bakker, G.J. (2008), *A finite element model for the deck of plate-girder bridges including compressive membrane action, which predicts the ultimate collapse load*
- Chamululu, Godfrey (2009), *Compressive membrane in slender bridge decks*
- Rooij, R.F.C. de (2010), *(Preliminary research) Compressive membrane action in transversally prestressed concrete decks*

Theory

Failure mechanism: bending

Theory of Park

The load deformation diagram of a laterally restrained rectangular reinforced concrete slab is shown in Figure A-1. The beneficial effect of CMA is here clearly illustrated. Important for CMA is that cracking is needed, else the compression stresses cannot develop.

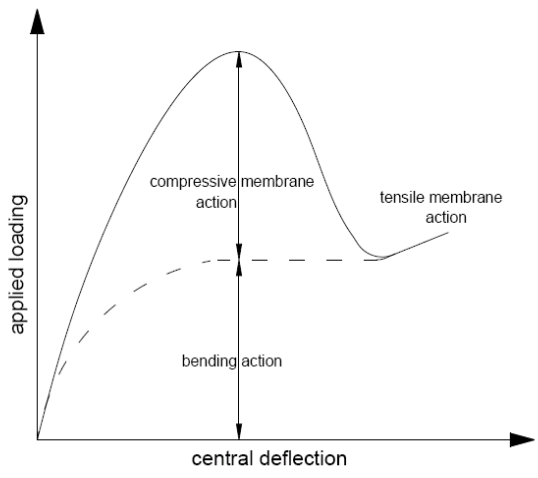

Figure A-1 Load deflection relationship

The transverse direction of the concrete slab is simplified to a one-way strip, that is restrained at both sides. The restraining is caused by the girders and the adjacent concrete. Figure A-2 shows the starting point for Park's CMA theory. The most important assumptions are that the system is symmetric and that rotations and translations are restrained at the supports.

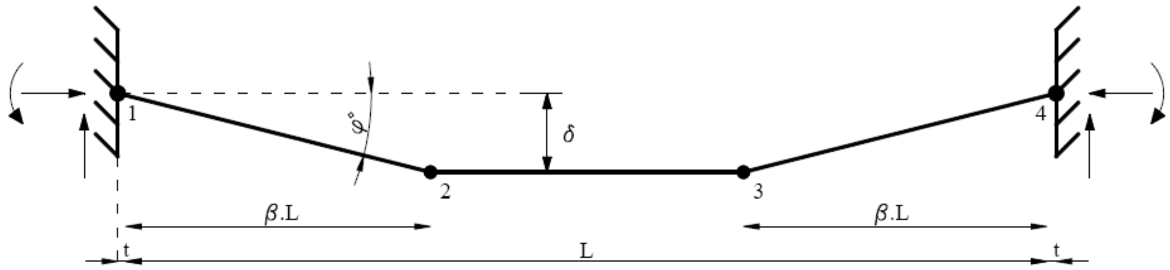

Figure A-2 Mechanism for Park's theory

From geometrical considerations the positions of the neutral axis in the plastic hinges can be solved. The deformed stage is visualised in Figure A-3.

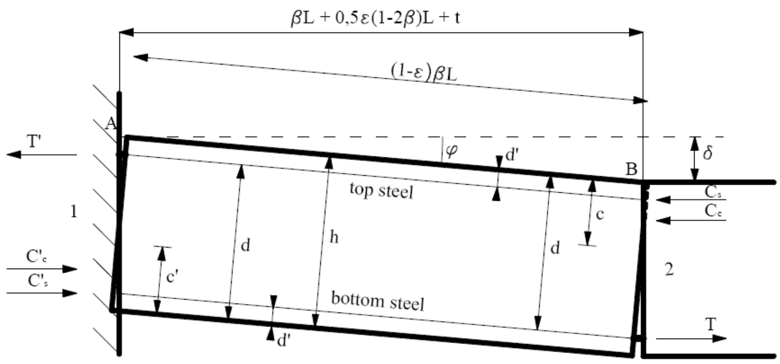

Figure A-3 Section 1-2 in deformed stage

The analytical solutions for the position of the neutral axis are:

$$c' = \frac{h}{2} - \frac{\delta}{4} - \frac{\beta L^2}{4\delta}\left(\varepsilon + \frac{2t}{L}\right) + \frac{T' - T - C_s' + C_s}{1{,}7 f_c' \beta_1}$$

$$c = \frac{h}{2} - \frac{\delta}{4} - \frac{\beta L^2}{4\delta}\left(\varepsilon + \frac{2t}{L}\right) - \frac{T' - T - C_s' + C_s}{1{,}7 f_c' \beta_1}$$

In Figure A-4 is shown how the forces are working in an section of the slab. β_1 is the ratio between the depth of the equivalent stress block (with value $0.85f'_c$) and the neutral axis depth. This factor depends on the compressive strength of the concrete.

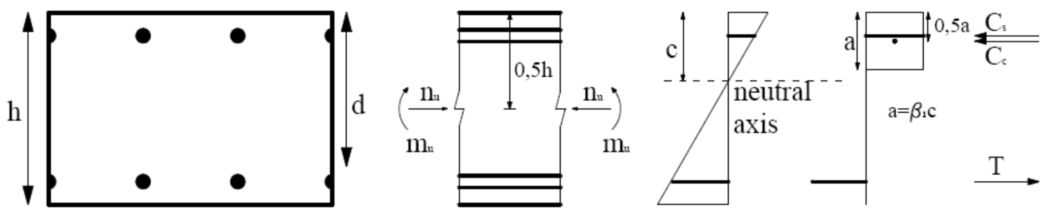

Figure A-4 Forces and moments in section

The forces n'_u and m'_u (left side) and n_u and m_u (right side) can be calculated. A sum of the moments around the mid-depth at one end of the strip is given by:

$$m_u' + m_u - n_u \delta$$

With the principal of virtual work the energy of the internal and external forces can be equated and a relation between the deflection δ of the strip and de load can be evaluated. The first part of the load-deflection curve is not correct because the plastic hinges are not immediate forming. So it's expected that the relationship is accurately only when sufficient deformation has occurred.

The influence of length, thickness, reinforcement ratio, concrete strength and steel strength are investigated by Bakker.[4] His conclusions are:

- The length is only of influence for short spans. The influence on the enhancement factor is rather small.
- The thickness of the slabs have a big influence on both enhancement factor and ultimate load.
- The higher the reinforcement ratio the smaller the enhancement factor.
- The higher the yield strength of the steel the lower the enhancement factor.
- For higher concrete strengths the enhancement factor and the ultimate load will increase both.

Enhancements by Miltenburg

Miltenburg made enhancements on the approach of Park by including the effects of prestressing force, creep, strain-hardening of the steel reinforcement, temperature changes and shrinkage. This advanced model is rewritten without prestressing because this is not the case for the bridge deck.

Elongation

For the derivation the beam is schematized in Figure A-5. This can be further simplified to the model in Figure A-6.

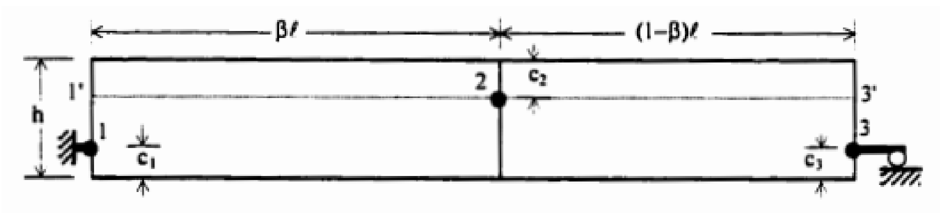

Figure A-5 Model of beam

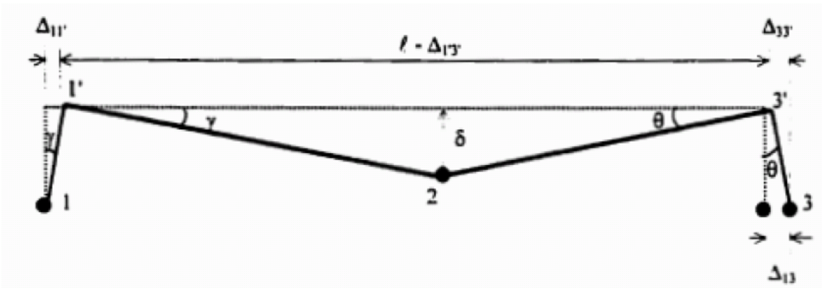

Figure A-6 Model of beam in deformed state

The total geometric elongation of the span length between the supports is given by:

$$\Delta_{13} = (h - c_2 - c_1)\frac{\delta}{\beta l} + (h - c_2 - c_3)\frac{\delta}{(1-\beta)l} - \frac{\delta^2}{2\beta(1-\beta)l}$$

4 Bakker, G.J. (2008), *A finite element model for the deck of plate-girder bridges including compressive membrane action, which predicts the ultimate collapse load*, page 11-13.

Shortening
Membrane action is of course sensitive to shortening. Therefore al kinds of shortening should be included.

The elastic strain at mid-depth of slab is:

Elastic strain: $\varepsilon_{Nu} = \frac{N_u}{EA}$ with axial stiffness: $EA = E_s A_s + E_c (A_c - A_s)$

The influences of creep, shrinkage and temperature changes also influence the length:

- Creep is included by Meamerian et. al. with a factor k. This factor is the ratio between long term and short term deformations. Because creep is dependent on axial force the strain can be expressed as: $\varepsilon_{cr} = k\varepsilon_{Nu}$
- Shinkage and temperature deformations must be included as separate strain: (ε_{S+T}).

Sum of effects

Total elongation: $$\Delta_{13} = (h - c_2 - c_1)\frac{\delta}{\beta l} + (h - c_2 - c_3)\frac{\delta}{(1-\beta)l} - \frac{\delta^2}{2\beta(1-\beta)l} - \left(\frac{(1+k)N_u}{(1+(n-1)\rho)E_c hb} + \varepsilon_{S+T}\right)l$$

Lateral restraint
To calculate the membrane action the the lateral restraint is of importance. The model is given in Figure A-7 whereby the to springs are combined to one spring at one side. Here the stiffness of the supports is considered.

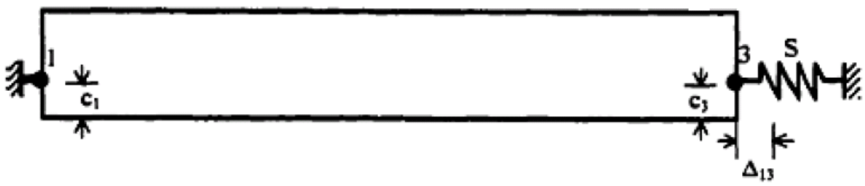

Figure A-7 Equivalent model of restraint

Reaction of the equivalent spring: $N_u = bS \cdot \Delta_{13}$.
(The width b is included because the elongation is given for a width and the spring stiffness S is given per unit width.)

Position of neutral axis
This is done following the CSA standard. The height of the concrete compression zone can be derived from: $C_{ci} = \alpha_1 f_c^{'} (\beta_1 c_i b - A_{si}^{'}), \qquad i = 1,2,3$

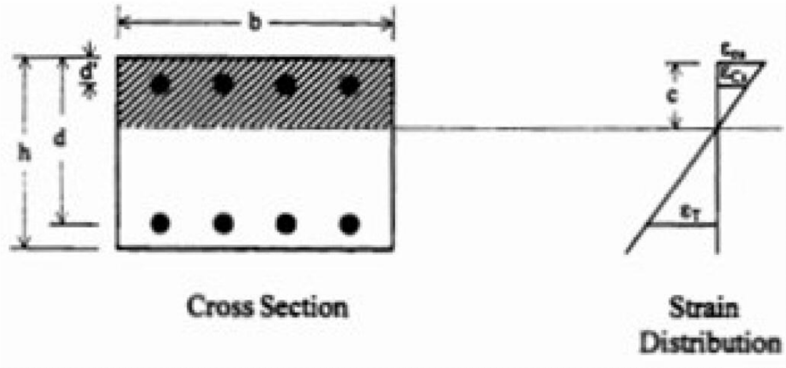

Figure A-8 Position neutral axis and strains in steel

The forces in the reinforcement steel can be derived with:

$\varepsilon_{Ti} = \varepsilon_{cu}\left(\frac{d_i - c_i}{c_i}\right)$ (tension side) and $\varepsilon_{Csi} = \varepsilon_{cu}\left(\frac{c_i - d'_i}{c_i}\right)$ (compression side)

With modified tri-linear idealization (Figure A-9) for mild steel the forces in the reinforcement can be derived using Hookes law.

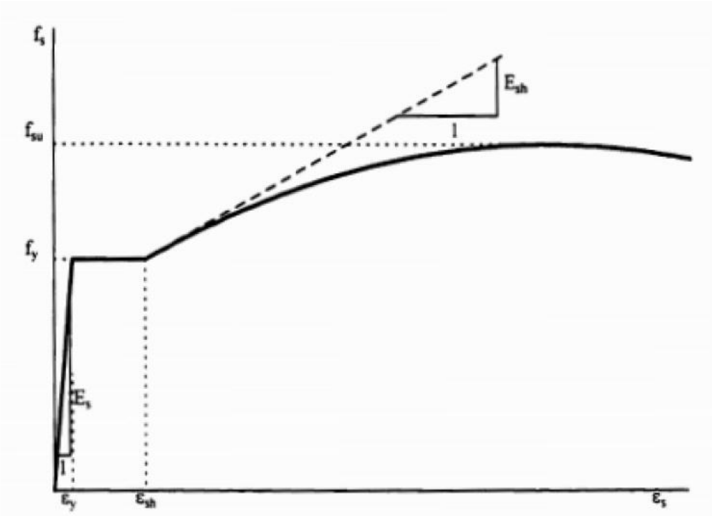

Figure A-9 Stress-strain relationship [Sargin, 1971]

Horizontal equilibrium

Now the sum of horizontal forces can be made to derive the location of the neutral axis. The huge expressions are given in the report of De Rooij. Interesting is the fact that in this expressions the prestressing doesn't play a role.

Finally a big expression is given which relates the displacement at the support with the forces (the force F_{ps} is removed from the equation):

$$\left(\frac{(1+k)N_u}{(1+(n-1)\rho)E_c hb} + \varepsilon_{S+T}\right)l + \Delta_{13} = \left[\frac{1}{1+\alpha_1 f'_c \beta_1 \frac{(1-\beta)\beta l}{2\delta}\frac{(1+k)l}{(1+(n-1)\rho)E_c h} + \frac{1}{S}}\right] \cdot$$

$$\left\{\left(\frac{(1+k)l}{(1+(n-1)\rho)E_c h} + \frac{1}{S}\right)\left[\alpha_1 f'_c \beta\left(\frac{h}{2} - \frac{\delta}{4} + \frac{(\beta-1)(T_1 - C_{s1}) + T_2 - C_{s2} - \beta(T_3 - C_{s3}) + \alpha_1 f'_c\left((\beta-1)A'_{s1} - A'_{s2} - \beta A'_{s3}\right)}{2\alpha_1 f'_c \beta_1 b}\right) + \frac{C_{s2} - T_2}{b}\right] + l\varepsilon_{S+T}\right\}$$

An iterative procedure is required to find the set of forces and locations of neutral axis with this formula.

After this the axial forces and moments can be derived from a sectional analysis. With help of Figure A-10 equilibrium equations can be derived for the left segment. This is also done for the right segment.

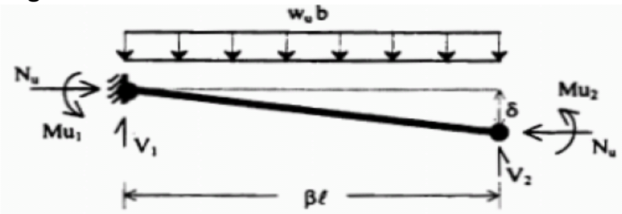

Figure A-10 Left segment of model

From this follows the formula: $$w_u = \frac{2}{bl^2}\left[\frac{M_{u1}}{\beta} + \frac{M_{u2}}{(1-\beta)\beta} + \frac{M_{u3}}{1-\beta} - \frac{N_u\delta}{(1-\beta)\beta}\right]$$ This formula can be solved iteratively.

Important is the position of the central hinge. The location can be found by solving the place where the derivative of w_u is zero.

Note: No idea is given about the stiffness of the supports.

Model Chamululu[5]

Chamululu proposed a theory based on the McDowell's masonry theory. In this model the behaviour of the strip is idealised as shown in Figure A-11. The two capacities are summed up to arrive at the total bearing capacity.

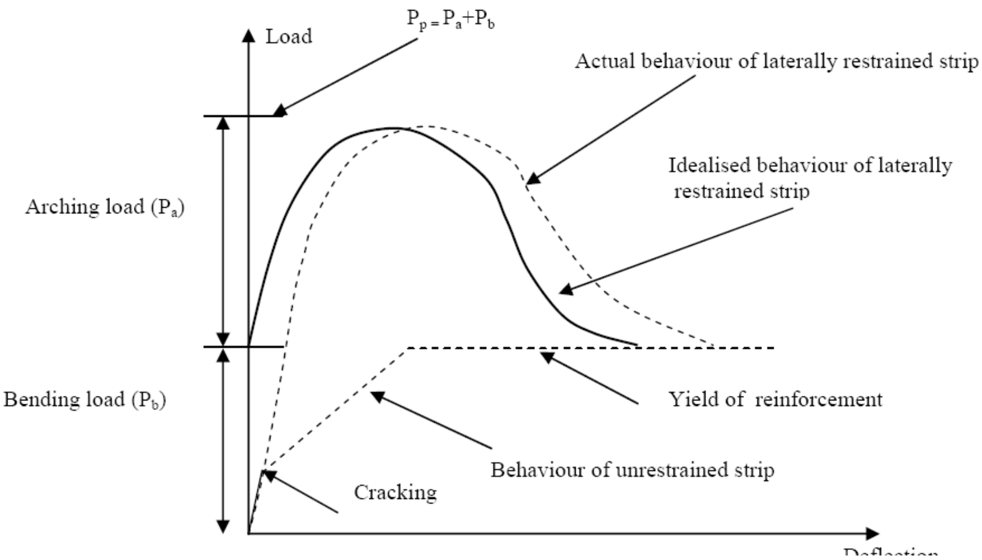

Figure A-11 Idealised behaviour of laterally restrained strip

This practical model isn't found back in other, later published, reports and therefore not further studied.

[5] Chamululu, Godfrey (2009), *Compressive membrane in slender bridge decks.*

Failure mechanism: punch

Plastic theory

The situation is given in Figure A-11

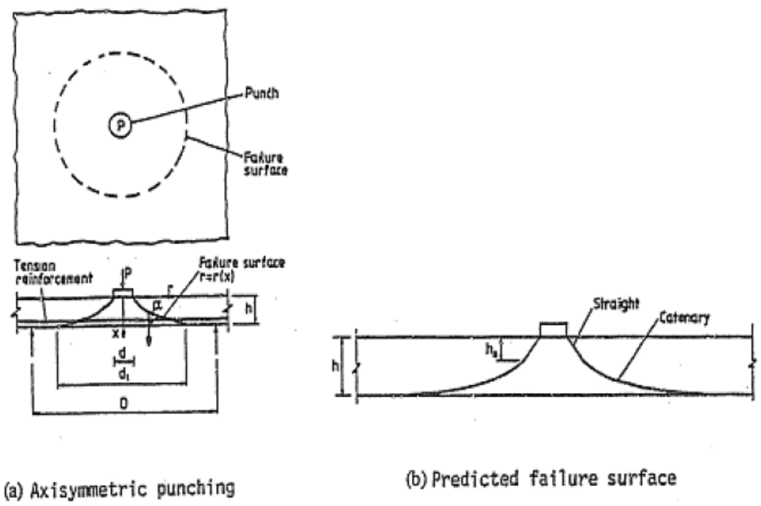

Figure A-12 Punching faillure model using plastic theory (Breastrup and Nielsen)

The basis of this theory is to equal the external and internal energy. Some solutions are given:

- Braestrup and Nielsen (1976): $Pu = \int_0^h \frac{1}{2} f_c u(l - m\sin\alpha) 2\pi r \frac{dx}{\cos\alpha}$
- Jiang and Shen (1986): $P = \pi f_t \left(\frac{d_1^2}{4} - \frac{d^2}{4} + \frac{2Kh^2}{\ln d_1 - \ln d} \right)$

A simplification of the formulation is also given by Jiang and Shen:
$P = 0{,}21 f_c sh$ with $s = \pi(d + h)$

The tests where done with concrete with a cast-in steel ring. Therefore some CMA was occurring. Due to this way of testing the plastic theory gives the failure load of prestressed deck slabs, for a certain range of prestressing, which is much higher than non-prestressed concrete decks.

Restraint factor concept

Hewitt and Batchelor proposed the usage of a restraint factor η to incorporate unspecified values of the axial forces and moments caused by lateral restraint. They used maximum possible values for these forces found by Brotchie and Holley.

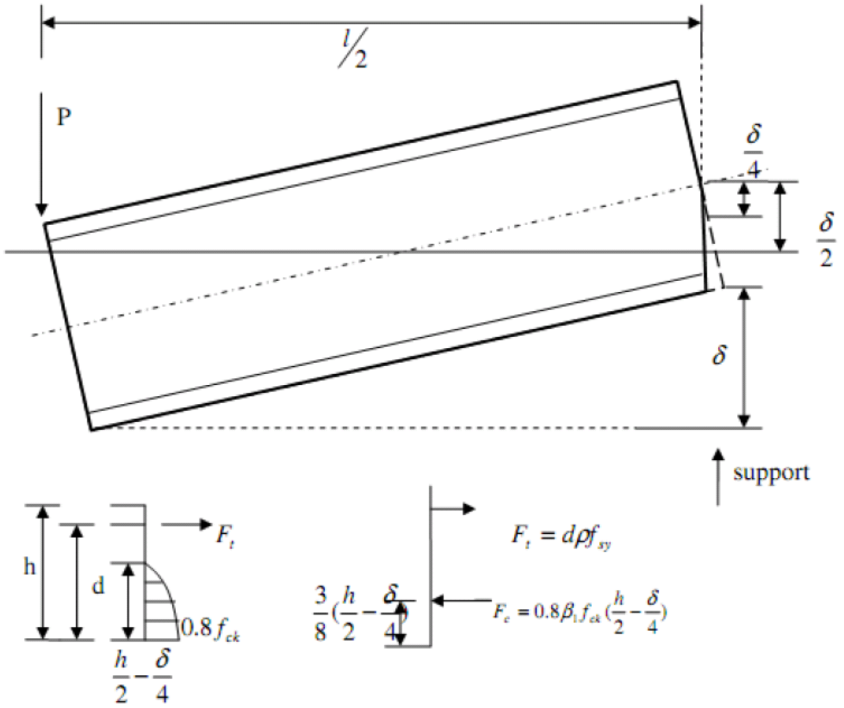

Figure A-13 Idealized displacement and boundary forces in the fully restraint slab

Maximum forces (fully restraint) from Brotchie and Holley:

$$F_{b(\max)} = F_c - F_t$$

$$M_{b(\max)} = F_t(2d - h) - F_c(d - 13h/16 - 3\delta/32)$$

Mean assumption of the model: For non-rigid boundaries it is assumed that the following schematization is possible:

$$F_b = \eta F_{b(\max)}$$

$$M_b = \eta M_{b(\max)}$$

There are some variants:

1. η=0.9, independent of the prestressing force.
2. η follows a linear line and is in relation with the occurring prestress level.
3. Value of F_p is equal to the occurring membrane force.
4. The restraint factor is a ratio of the prestressing force and maximum force: $\eta = \dfrac{F_p}{F_{b(\max)}}$

Punching failure model and analysis

A portion bounded by shear and radial cracks is considered in this analysis (Figure A-14).

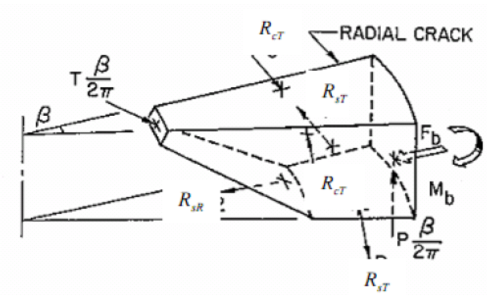

Figure A-14 Forces on sector element

There is a set of implicit equations which can be solved with a computer program. It is not of that importance to present all equations.

Comparison bending and punch

The two different failure modes (bending and punch) both include a kind of stiffness of the supports. The bending model with a physical support stiffness and the punching model with a dimensionless restraint factor. Therefore a direct comparison is not possible, the punching model was adapted by Wei[6] to compare the results.

Wei proposed a value for the lateral stiffness: $S_t = 0.48 c_t \dfrac{E_c A_c}{c}$ with $c_t = 100\rho\sqrt{\dfrac{h}{200}}$

From the report of Wei also follows that for a square concrete slab with a concentrated load always the punching capacity is governing.

From the report of Chamululu[7] follows that the enhancement due to CMA for the bending mode is much larger than that of the punching mode.

Bakker[8] gives a comparison from which follows that for low slenderness punch is governing. He didn't define 'low slenderness'.

In the report of Bae[9] one of the conclusions is that the failure mode depends on the lateral restraint. With sufficient lateral restraint punching failure will occur. Without sufficient lateral restraint a flexural failure or snap through instability can occur.

From tests follows that nearly always the punching failure is the governing failure mode.

[6] Wei, Xuying (2008), *Assesment of real loading capacity of concrete slabs,* page 90.
[7] Chamululu, Godfrey (2009), *Compressive membrane in slender bridge decks.*
[8] Bakker, G.J. (2008), *A finite element model for the deck of plate-girder bridges including compressive membrane action, which predicts the ultimate collapse load*, page 20.
[9] Bae, Han-Ug (2008), *Design of reinforcement-free bridge decks with wide flange prestressed precast girders,* Page 206.

Codes

New Zealand[10]

Design loading

Loads:

- (Superimposed) Dead load
  - Weight of structural members.
  - All permanent loads added.
  - A minimum allowance of 0.25 kN/m^2 should be applied for future services.
- HN (normal)
  - A strip of 3 meter width with a load of 3.5 kN/m^2 (10.5 kN/m devided by 3 meter).
  - Pair of axle loads of 120 kN each spaced at 5 meter, on worst location.
  - Area wheel 500 x 200 mm^2.
- HO (overload)
  - Same uniform distributed load as for HN
  - Pair of axle loads of 240 kN each spaced at 5 meter, on worst location. Two alternative wheel contact areas are possible, take most negative one.
- Accident load
  - HN wheel load factored by dynamic factor.
  - Wheel positioned at the outer edge of the slab or kerb.

Load position:

- Loads applied within each load lane.
- Roadway includes carriageway and shoulders. Roadway is bounded by either the face of a kerb or the face of a guardrail or other barrier.

Load combination:

- Normal live load: HN loading shall be placed.
- Overload: HO loading shall be placed.
- Improbability of concurrent loading: factor taking into account number of elements in the load case. This is applicable to HN and HO.

Load groups for ULS, without effects like temperature, settlement etc.:

- Group 1A: $U = 1.35 \cdot (DL + 1.67 \cdot (LL \cdot I))$
- Group 2A: $U = 1.20 \cdot (DL + LL \cdot I)$
- Group 4: $U = 1.35 \cdot (DL + 1.10 \cdot (OL \cdot I))$

(DL: dead load, LL: live load, OL: overload, I: dynamic load factor)

Dynamic load factor:

- Must be applied for HN and HO and is dependent on material and location of the member being designed (graph).

Fatigue:

- Shall represent the expected service loading over the design life of the structure.
- No standard fatigue load spectrum available: use BS5400: Part 10: 1980 clause 7.2.2

[10] *New Zealand Bridge Manual* (september 2004)

Limitations and requirements
When limit's are not met of for cantilevers elastic plate bending analysis shall be used. The requirements are written two times in the code (in clause 4.2.2 and 6.5.2). Clause 4.2.2 gives rules for design, clause 6.5.2 rules for evaluation. The rules for design are relevant for this thesis.

- There are at least three longitudinal girder webs in the system.
- The deck is fully cast-in-place.
- The deck is of uniform depth.
- The deck is made composite with the supporting structural components.
- The core depth is not less than 90 mm (core depth = depth – top and bottom covering)
- Diaphragms at supports (for reinforced and prestressed concrete girders).
- The supporting components are made of steel or concrete.
- The ratio of the span length to slab thickness should not exceed 15. For skew slabs the skew span shall be used (L_s/cos(angle)).
- The maximum slab length does not exceed 4 meter. For skew slabs the skew span shall be used (L_s/cos(angle)).
- The minimum slab thickness is not less than 165 mm.
- The overhang beyond the centreline of the outside beam should be at least 5 times the slab thickness.
- The specified 28 day compressive strength of the deck concrete is not less than 30 MPa.

For skewed slabs with angles greater than 20° in the end region 0.6% reinforcement must be placed, while the minimum is 0.3%. See Figure A-15 for an illustration of the reinforcement.

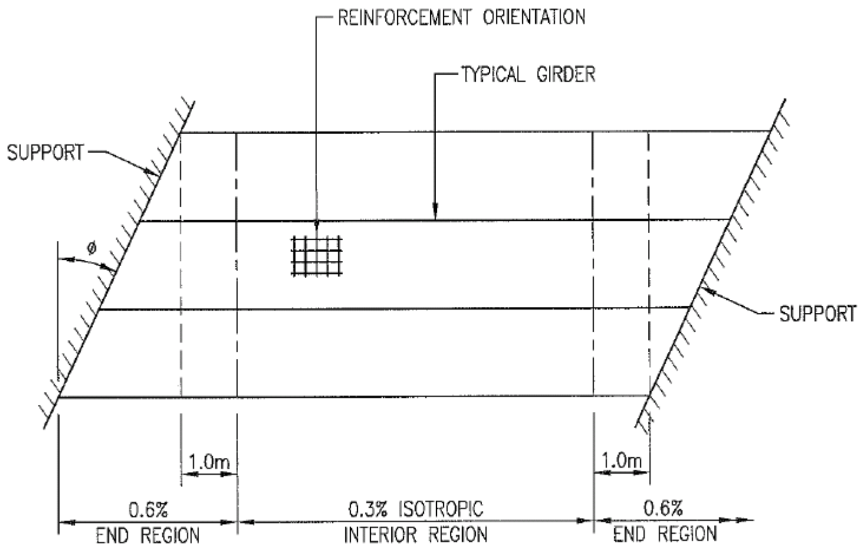

Figure A-15 Reinforcement in skewed slabs by the empirical method

Evaluation
There are two possibilities for evaluation:

1. Rating: define bridge capacity using overload load factors or stress levels (overweigh vehicles)
2. Posting: define bridge capacity using live load factors or stress levels (conforming vehicles)

Because the normal use will be considered the posting procedure will be presented here.

Posting
The formula for live load capacity is:

Allowable Axle Load (kg)

$$= \left[\frac{Liveload\ wheel\ load\ capacity}{Posting\ load\ effect} x\ 8200\right]_{min}$$

$$= \left[\frac{\phi x(0.6R_i)}{\gamma_L x\, 40\ x\ I} x\ 8200\right]_{min}$$

Important:

- $\phi = 0.90 \cdot \phi_D$ (Good or fair, table 6.6) with $\phi_D = 0.5$ (6.5.2.b)
- The values from the charts shall be multiplied by 0.6 (6.5.2.b)
- R_i = section strength (from figure 6.1-6.5)
- $\gamma_L = 1.90$ (table 6.3)
- I = 1.3 (dynamic load factor for slabs, figure 3.2)
- Effects of dead load and other loads are neglected (6.5.2.b)

Canada[11]

Design loading[12,13]

Loads:

- Permanent loads
    - Dead loads (D)
    - Secondary prestress effects (P)

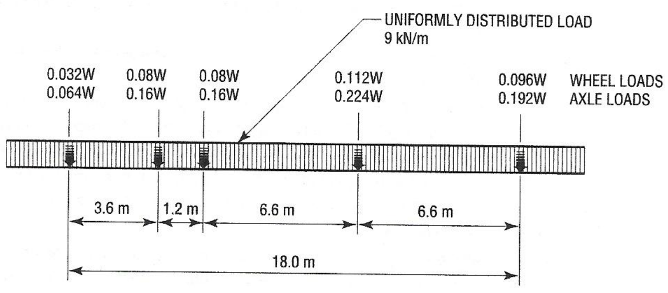

Figure A-16 CL-W Lane Load distribution

- Live load (Figure A-16)
    - 80% of CL-625 Truck
    - A strip of 3 meter width with a load of 3 kN/m^2 (9 kN/m devided by 3 meter). Don't apply when it's beneficial.
    - Area wheel 250 x 250 mm^2 (first axis) other axis 600 x 250 mm^2.

Load position:

- Loads applied within each load lane.
- Roadway includes carriageway and shoulders. Roadway is bounded by either the face of a kerb or the face of a guardrail or other barrier.

Load groups for ULS, without effects like temperature, settlement etc.:

- Load factors from Table A-1.

[11] Fang, I.K. et. al. (1986), *Behaviour of Ontario type bridge decks on steel girders*, page 4-6
[12] Chad, Andrew (2011), *Design of Slab- on-Girder Highway Bridges According to CAN/CSA-S6-00*
[13] Taylor&Francis Group (2000), *Bridge Loads*, chapter 4.4

3.5.1 (a) Load Factors and Load Combinations

	Permanent Loads			Transitory Loads					Exceptional Loads			
Loads	*D*	*E*	*P*	L^5	*K*	*W*	*V*	*S*	*EQ*	*F*	*A*	*H*
Fatigue Limit State												
FLS Combination 1	1.00	1.00	1.00	1.00	0	0	0	0	0	0	0	0
Serviceability Limit States												
SLS Combination 1	1.00	1.00	1.00	0.90	0.80	0	0	1.00	0	0	0	0
SLS Combination 2[2]	0	0	0	0.90	0	0	0	0	0	0	0	0
Ultimate Limit States[1]												
ULS Combination 1	α_D	α_E	α_P	1.70	0	0	0	0	0	0	0	0
ULS Combination 2	α_D	α_E	α_P	1.60	1.15	0	0	0	0	0	0	0
ULS Combination 3	α_D	α_E	α_P	1.40	1.00	0.50[4]	0.50	0	0	0	0	0
ULS Combination 4	α_D	α_E	α_P	0	1.25	1.65[4]	0	0	0	0	0	0
ULS Combination 5	α_D	α_E	α_P	0	0	0	0	0	1.00	0	0	0
ULS Combination 6[3]	α_D	α_E	α_P	0	0	0	0	0	0	1.30	0	0
ULS Combination 7	α_D	α_E	α_P	0	0	0.90[4]	0	0	0	0	1.30	0
ULS Combination 8	α_D	α_E	α_P	0	0	0	0	0	0	0	0	1.00
ULS Combination 9	1.35	α_E	α_P	0	0	0	0	0	0	0	0	0

Table A-1 Load Factors and Load Combinations

Dynamic load factor (Cl. 3.8.4..5.3):

- 0.50 for deck joints
- 0.40 where only one axle of the CL-W truck is used, except for deck joints.
- 0.30 where any two axles of the CL-W truck are used, or axles 1,2 and 3 are used; or
- 0.25 where three axles of the CL-W truck, except for axles 1,2 and 3 or more than 3 axles used.

Reduction factors:

- A reduction factor when there are more lanes Table A-2.

Number of Loaded Design Lanes	Modification Factor
1	1.00
2	0.90
3	0.80
4	0.70
5	0.60
6 or More	0.55

Table A-2 Modification factors for Multilane Loading

Fatigue:

- Special fatigue limit state (Table A-1).

Limitations and requirements

From clause 7.8.5.2 follows:

- A minimum of 0.3%, especially for SLS, not necessary for ULS. Only small haircracks occur.
- The girder space should not exceed 3.7 m.
- The cantilever should at least extend 1 m beyond the centreline of the exterior beam. Also the curb can be used but the cross-sectional area must be at least the same.
- The span length to thickness ratio should not exceed 15. For skew slabs, use skew span.
- For skew angles greater than 20° the end portions of the deck slab shall be provided with 0.6% isotropic reinforcement.

- Slab thickness not less than 225 mm (increased, in previous codes 190 mm, increased for durability) and spacing of isotropic reinforcement bars not exceed 300 mm.
- Diaphragm beams at supports.
- Spacing of shear connectors in composite system should not exceed 0.6 m.
- Edge stiffening for all slabs.

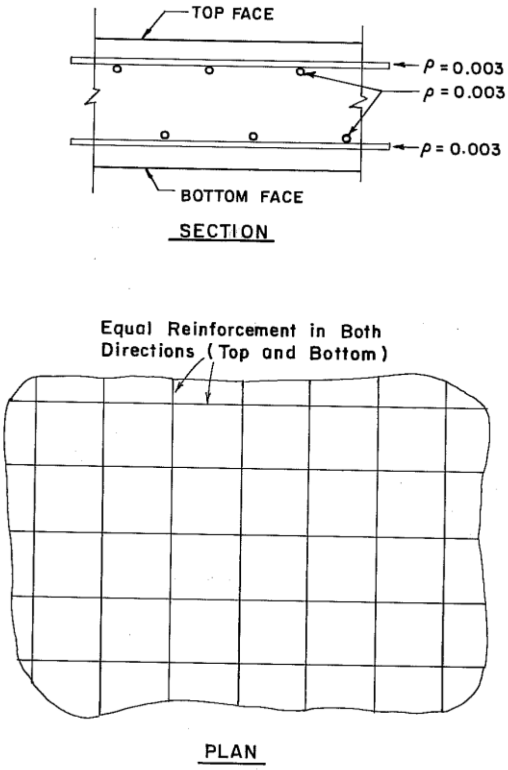

Figure A-17 Reinforcement plan prescribed by empirical method

Evaluation

The basic equation for punching shear is: $0.65 \cdot R \geq 1.20 \cdot D + 1.40 \cdot (1 + i) \cdot L$

Where:
- R: failure load [kN]
- D: dead load effect – about $0.20 \cdot L$ [kN]
- i: impact, 0.45 [kN]
- L: live load effect [kN]

The equation is then: $0.65 \cdot R \geq 1.20 \cdot 0.20 \cdot L + 1.40 \cdot (1 + 0.45) \cdot L = 2.27 \cdot L \rightarrow R \geq 3.49 \cdot L$

In the procedure it is assumed that crack control requirements and shear resistance requirements are met.

United Kingdom[14]

Design loading[15,16]

Loads:

- (Superimposed) Dead load
    - Weight of structural members.
    - All permanent loads added.
- HA (normal), calculated for 'loaded length'
    1. UDL (from figure 5.1 BD 21/01, function for W) and a KEL of 120 kN (Length < 50 m)
    2. A single axle load (Length < 2 m)
    3. A single wheel load of 100 kN (Length < 2 m), circular 340 mm or square 300 mm.
- HB (overload)
    - Special cases.
- Accident load
    - A single appropriate accidental vehicle shall be selected.
    - Wheel positioned at the outer edge of the slab or kerb.

Load position:

- Loads applied within each load lane.
- Roadway includes carriageway and shoulders. Roadway is bounded by either the face of a kerb or the face of a guardrail or other barrier (5.6).
- Width of carriageway between 2.5 m and 3.65 m (See Table A-3).

Carriageway Width (m)	Number of Notional Lanes
below 5.0	1
from 5.0 up to and including 7.5	2
above 7.5 up to and including 10.95	3
above 10.95 up to and including 14.6	4
above 14.6 up to and including 18.25	5
above 18.25 up to and including 21.9	6

Table A-3 Number of Notional Lanes

Load factors and combinations follows from Table A-4 and Table A-5.

Load	Limit State	γ_{fL} to be considered in combination				
		1	2	3	4	5
Dead: Steel	USL	1.05	1.05	1.05	1.05	1.05
	SLS	1.00	1.00	1.00	1.00	1.00
Dead: concrete	USL	1.15	1.15	1.15	1.15	1.15
	SLS	1.00	1.00	1.00	1.00	1.00
Superimposed dead: deck surfacing	USL	1.75	1.75	1.75	1.75	1.75
	SLS	1.20	1.20	1.20	1.20	1.20
Superimposed dead: other loads	USL	1.20	1.20	1.20	1.20	1.20
	SLS	1.00	1.00	1.00	1.00	1.00
Reduced load factor for dead & superimposed dead load where this has a more severe total effect	USL	1.00	1.00	1.00	1.00	1.00

[14] BD 81/02 (may 2002), *Use of compressive membrane action in bridge decks.*
[15] BD 21/01 (may 2001), *The assessment of highway bridges and structures,* Chapter 5.
[16] Olffen, Bram van, *Interactive Course Concrete Bridges,* page 57.

Table A-4 Load combinations and factors for permanent loads

Load		Limit State	γ_{fL} to be considered in combination 1	2	3	4	5
Highway: live loading	HA alone	USL	1.50	1.25	1.25		
		SLS	1.20	1.00	1.00		
	HA with HB or HB alone	USL	1.30	1.10	1.10		
		SLS	1.10	1.00	1.00		
	footway and cycle track loading	USL	1.50	1.25	1.25		
		SLS	1.00	1.00	1.00		
	accidental wheel loading	USL	1.50				
		SLS	1.20				

Table A-5 Load combinations and factors for live loads

Dynamic load factor:

- Must be applied for HN and HO and is dependent on material and location of the member being designed (graph).

Reduction factor:

- K = Assesment live loading / Type HA loading. Only for loaded lengths above 2 m.
- Factor AF for different span ranges to account for lateral bunching effect. The HA UDL and KEL are calculated with this effect but at high speed no lateral bunching is the most onerous criterion for bridge loading. Therefore divide by this factor (5.23 BD 21/01).
- Lane factor (5.24 BD 21/01).
  - Lane 1 1.0
  - Lane 2 1.0
  - Lane 3 0.5
  - Lane 4 0.4

Fatigue:

- Shall represent the expected service loading over the design life of the structure.
- Use BS5400: Part 10: 1980 clause 7.2.2

Limitations and requirements

- (3.6) Slab at least 160 mm thick.
- (3.6) At least grade 40 (characteristic compressive strength after 28 days) concrete.
- (3.6) The local strength may be assumed adequate for up to 45 units of HB.
- (3.11) Deck slab reinforcement shall be derived in accordance with BD 24 on basis of global effects only.
- (3.11) The resistance to local affects shall be derived from 5.2-5.9 (punching included).
- (3.12) Without adequate boundary restraint the effects of the global and local effects shall be derived from the direct strain due to global effects combined with the flexural strain due to local effects in accordance with BD 24.
- (3.13) Minimal reinforcement 0.3%. Spacing not greater than 250 mm. Not less than 750 mm^2/m
- (5.10) Span of slab panel should not exceed 3.7 m.
- (5.10) The slab shall extend at least 1.0 m beyond the centre line of the external longitudinal supports. Or use kerb.
- (5.10) The span length to thickness ratio should not exceed 15. Skew slabs: skew spans.
- (5.10) For skew angles greater than 20° end portions of deck in accordance with BD 24 and 44.
- (5.10) Transverse edges at ends of bridge or at supports should be supported by diaphragms or other suitable means.
- (5.10) Diaphragms at support lines of all bridges. For prestressed beams only at the ends.
- (5.10) All slabs having main reinforcement parallel to traffic should have edge beams.

Evaluation

The method assumes that the slab reinforcement makes no contribution to the local load carrying capacity.

Notation:

d average effective depth to the tensile reinforcement (mm)

f_{cu} characteristic concrete cube strength (N/mm^2)

h overall slab depth (mm) (for precast concrete participating formwork panels, to allow for the reduced depth at panel joints, h shall be taken as the overall depth minus 10 mm)

L_r half span of slab strip with boundary restraint (as defined in 1.8) (mm)

γ_M = partial safety factor for strength

φ = diameter of loaded area (mm)

Concrete compressive strength:

$$f_c = \frac{0.8 f_{cu}}{\gamma_m} \qquad \text{Equation 1}$$

The plastic strain of an idealised elastic-plastic concrete is given by:

$$\varepsilon_c = (-400 + 60 f_c - 0.33 f_c^2) \times 10^{-6} \qquad \text{Equation 2}$$

Non-dimensional *parameter* for arching moment of resistance (R), must be less then 0.26 to apply CMA:

$$R = \frac{\varepsilon_c L_r^{\ 2}}{h^2} \qquad \text{Equation 3}$$

Non-dimensional arching moment *coefficientI:*

$$k = 0.0525\,(4.3 - 16.1\sqrt{3.3x10^{-4} + 0.1243R}) \qquad \text{Equation 4}$$

Effective reinforcement ratio:

$$\rho_e = k\left[\frac{f_c}{240}\right]\left[\frac{h}{d}\right]^2$$

Ultimate predicted load for a single wheel:

$$P_{ps} = 1.52(\varphi + d)d\sqrt{f_c}\,(100\rho_e)^{0.25} \qquad \text{Equation 6}$$

For axle loading (two wheels on one slab or two wheels on adjacent axles):

$$P_{pd} = 0.65P_{ps} \qquad \text{Equation 7}$$

Modelling concrete

Introduction

It's important to make an argued choice for a model. For that reason the reports of other master students were studied to tackle the most important problems.

Information from other reports

Report Han-Ug Bae

Han-Ug Bae did also a FE analysis. He used, beside other models, the model showed in Figure A-18.

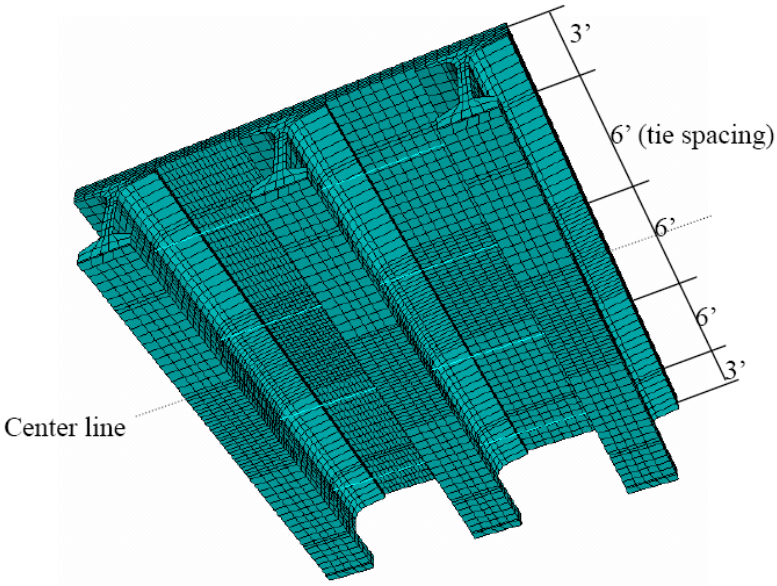

Figure A-18 Modelling of the bridge for parameter study

Report Bakker

For membrane action cracking is important. For bending a 2D-model will be sufficient, for punching a 3D-model is necessary. Load steps can be applied in two different ways, by displacements or by forces.

Way of modelling

Bakker compared five different FE-models. It was shown in his study that the 2D beam model and 3D shell model give almost the same results. The same conclusion holds for the results obtained with the 2D plane stress and the 3D solid model. An overview of the found results is given in Table A-6.

	input	graphical output	realistic model	punch behaviour	calculation time
2D beam model	++	--	+	irrelevant	++
2D plane stress model	+	+	+	irrelevant	+
3D curved shell model	o	-	+	--	o
3D solids model	-	++	++	o	--
axi-symmetric model	+	+	-*	++	+

* : rectangular slabs cannot be modelled with this model

Table A-6 Overview of different FE models and their results

Cracking

There are two cracking models possible, smeared cracking or total strain cracking. Smeared cracking depends on principal stresses.

The total strain crack model describes the tensile and compressive behaviour of a material with one stress-strain relationship. Within both rotating or fixed cracking this model can be chosen. The difference is that for fixed cracking the cracks lies in the same direction for all the load steps, while by rotating cracking, the direction of the crack is calculated separately for each load step.

Bakker applied the total strain rotating crack model and the direction of the cracks varied for each load step.

Concrete in tension - Post-cracking behaviour
The Dutch code is based on models with brittle cracking, but including tension softening may give result, that lie closer to the real collapse load. Bakker used both the brittle and Hordijk model.

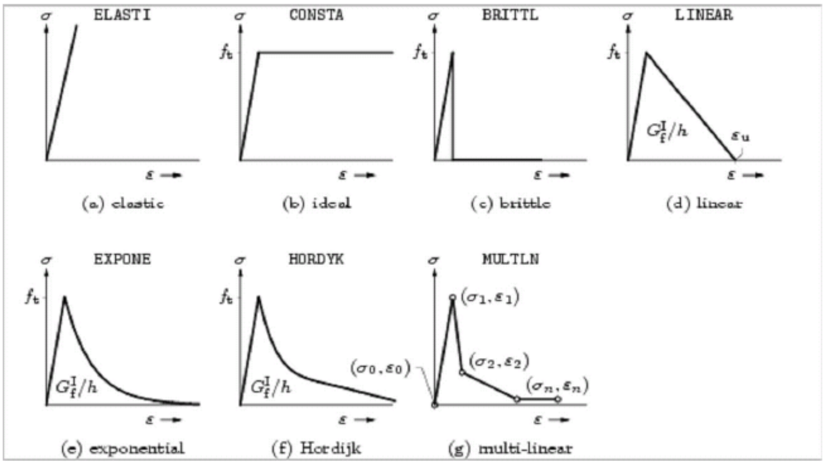

Figure A-19 Different models for concrete behaviour after cracking

Concrete in compression
Bakker used the ideal elasto-plastic model in his calculations.

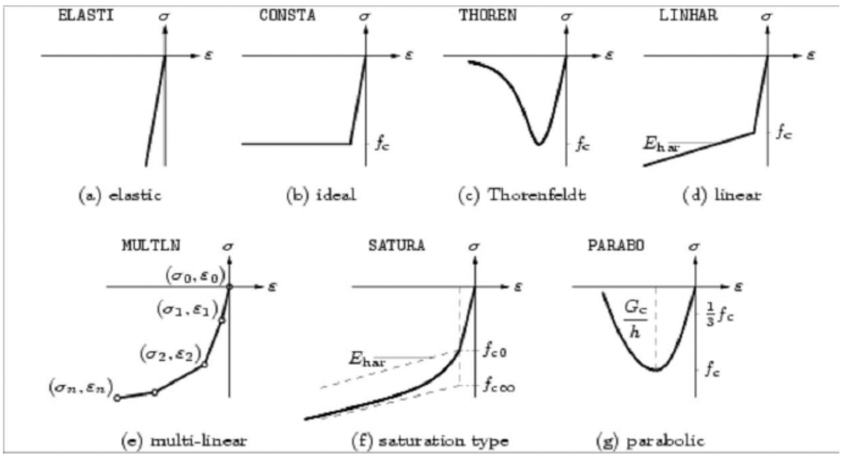

Figure A-20 Concrete behaviour under compression

Reinforcement
For the reinforcement there are three options, ideal plastic, a work-hardening diagram or a strain-hardening diagram. The ideal plastic model is used.

Model
The models that Bakker used:

- Total strain rotating crack model.

- Both brittle and Hordijk tension softening in tension
- Ideal plastic model in compression
- Ideal plastic model for the reinforcement

FEM for bending action
Bakker used the 2D plane stress model to analyse the stresses.

The brittle material model gives slightly less enhancement factor than the model with tension softening.

From comparison with test results Bakker concluded that the brittle model seems to give a better approximation of the collapse load than the tension softening model.

The tension softening model is much more ductile than the brittle model.

The brittle model needs more iterations to reach its convergence criterion in each step. For a fully 3D solids model this will be something to keep in mind.

FEM for punching failure
Bakker used the 3D plane stress model or the axi-symmetric model.

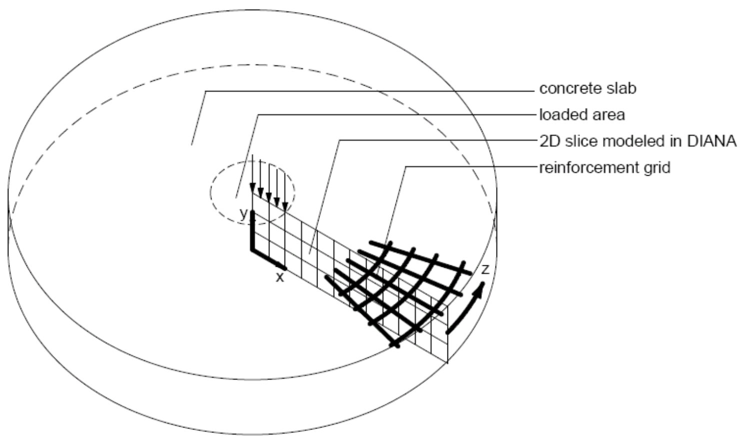

Figure A-21 Axi-symmetric model

Four models where compared:
- Brittle material model, all sides simply supported
- Brittle material model, all sides clamped
- Tension softening material model, all sides simply supported
- Tension softening material model, all sides clamped

For the brittle model the collapse load was already reached before punching occurred.

After this Bakker applied the axi-symmetric model. With this model big differences in ultimate load capacity were found when the brittle or tension softening material model was applied. The conclusion was that the axi-symmetric model with brittle material behaviour is the fastest and best.

Report Minalu
Minalu compared different modelling techniques:

Orthotropic plate model
An equivalent slab is calculated with different stiffness in both directions. The transverse stiffness of the beams is neglected. Minalu calculates this model with SCIA Engineer with a Mindlin plate element.

Limitations:
- The modelling technique fails to deal with the following aspects of bridge deck behaviour: transverse and longitudinal in plane forces, distortion of beam members, local bending effects.
- The different position of the neutral axis in the transverse direction of the bridge is not taken into account.
- Location of support system is normally under the beams, but in the model the supports are located at the neutral axis.

Centric beam elements for the girders and plate bending elements for the deck
The deck slab has been modelled by using quadrilateral plate bending elements. The precast prestressed girders and end diaphragms have been idealized using beam elements. The centroid of each of the girders and diaphragm coincided with the centroid of the concrete slab. SCIA Engineer commercial finite element software package is adopted for this model.

Limitations:
- The following things cannot be taken into account: transverse variation in the level of the neutral axis, transverse and longitudinal in-plane forces.
- Model fails to consider distance between the centre of the deck and girders: underestimation of flexural strength.
- Location of support system is normally under beams, but in the model at the neutral axis.

Eccentric beam elements for the girder and shell elements for the deck.
The eccentricity of the beams is realised with a rigid vertical member. This is also possible with SCIA Engineer. With this model tension in the deck was found.

Shell elements for both the deck and the girders
Some approximations had been done to couple the beam to the slab. The approximation increases the bending and torsion inertias of the girders. Hence, this model predicted higher torsion moments.

Limitations:
- SCIA Engineer failed to connect the shell elements of the deck with the shell elements of the beams by a rigid link.

3D model with volume elements
Minalu used ATENA 3D. ATENA 3D is especially designed to simulate real behaviour of concrete and reinforced concrete structures including concrete cracking, crushing and reinforcement yielding. Geometrical and physical non-linear analysis is also possible in ATENA 3D. In this case study, 3D linear elastic analysis has been carried out using standard brick elements. To decrease computational time first order linear interpolation elements were employed. The cracking of the structure was incorporated by reducing the stiffness of the elements.

For the reduction of the torsion stiffness two solutions are possible:

- Reduction of torsion moment of inertia: not possible for shell and volume finite elements.
- Reduction of the shear modulus: in ATENA 3D is was not possible to change the shear modulus keeping the modulus of elasticity and poison’s ratio unchanged. Consequently Minalu only investigated SLS with full torsion stiffness.

Limitations:

- In ATENA 3D it is impossible to create an orthotropic deck having different stiffnesses in the transverse and longitudinal direction. To consider the effect of cracking for the deck slab half of young’s modulus was used in both directions for all finite element models.

B. Comparison calculation skew and straight bridges

Objective

Two calculations are made to have a starting point for the 3D models.

Comparison

The most important parameters of the bridges are compared. One of the first figures in the report of Minalu was about the load distribution in a skew bridge and is shown in Figure B-1. Minalu also made an analysis of the effect of skewness on the load distribution.[17] The differences found between the straight and skew bridge are compared with his conclusions.

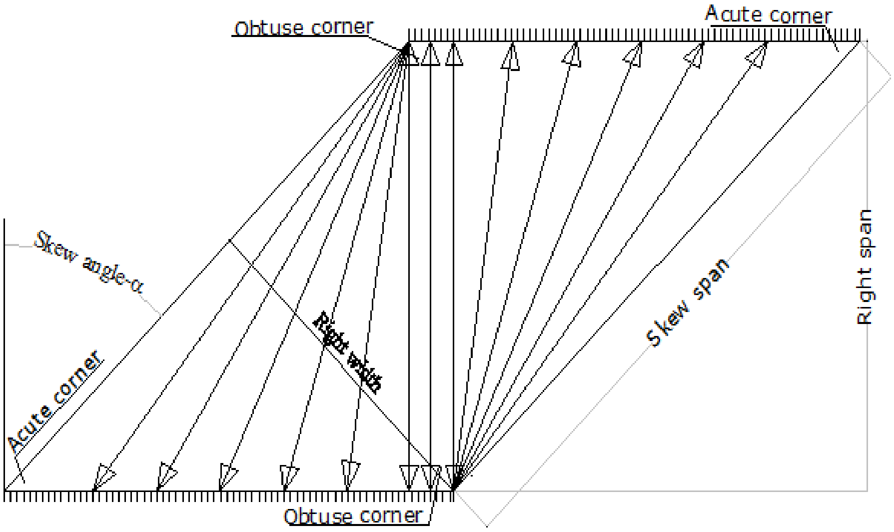

Figure B-1 Load paths in torsion stiff skew bridges[18]

Note: Minalu also calculates an orthotropic plate model, so the absolute values should be the same. This is not the case due to a small mistake in the calculation. Minalu applied the supports correctly at some distance from the ends of the girder, but didn't specify the distance in his report. In the model used for the calculations presented in this report the supports where placed at the ends of the girders, which is physically impossible. So the span between the supports was 36 m instead of 35.3 m, assuming that Minalu used a 0.35 m distance. This will give higher longitudinal moments. However, in the calculation of the cross-section in the program Span the correct span was used. So finally the mistake will not have big impact for the prestressing. In the model however there will be little deviation in the values.

Note: the stiffness matrix of Minalu differs with the stiffness matrix used for the calculations of this report. Parameter D11 is much bigger in this report. That will give some differences in load distribution, the longitudinal direction will attain a bigger part of the load. Also the used matrices in the models of Minalu do not correspond with the matrices presented in his report.

Longitudinal moment in girders

The applied loads are given in Figure B-2.

[17] Minalu, Kassuhun K. (2010), *Finite element modelling of skew slab-girder bridges.* Page 100-106.
[18] Minalu, Kassuhun K. (2010), *Finite element modelling of skew slab-girder bridges.* Page 2.

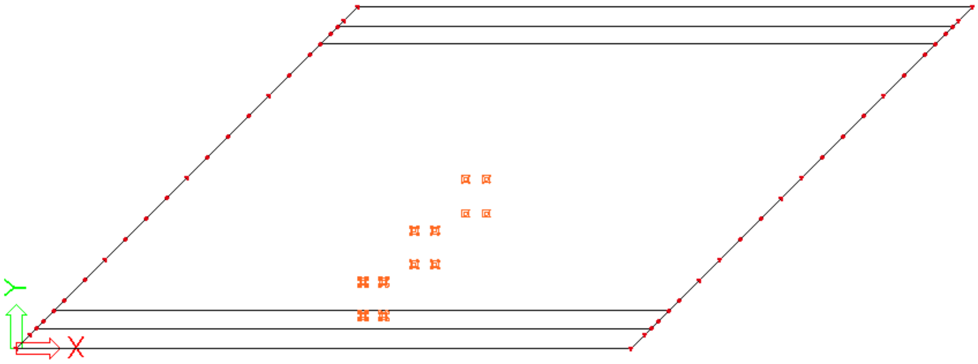

Figure B-2 Loads for maximum longitudinal moment (with corresponding negative working lane loads)

From this load case follows governing moments, presented in Table B-1.

Girder	Straight bridge [kNm]	Skew bridge [kNm]	Deviation [%]
ZIP	3524.3	3430.6	-2.65
1^{st} ZIP	3387.4	3339.5	-1.41
TRA	2467.9	2435.2	-1.33

Table B-1 Comparison longitudinal moment

The differences are negligible. Minalu also found a reduction in longitudinal bending moment in the first ZIP, but in his case this reduction was larger: -3.83 %.

Transversal moment in deck

The applied loads for the negative and positive moments in the deck are given in Figure B-3 and Figure B-4.

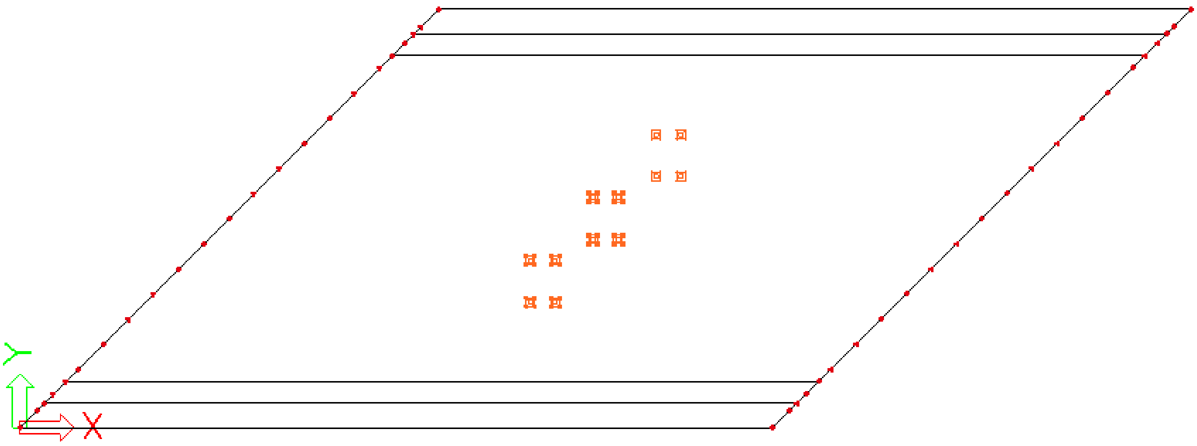

Figure B-3 Applied axle loads for maximum positive moments (with corresponding lane loads)

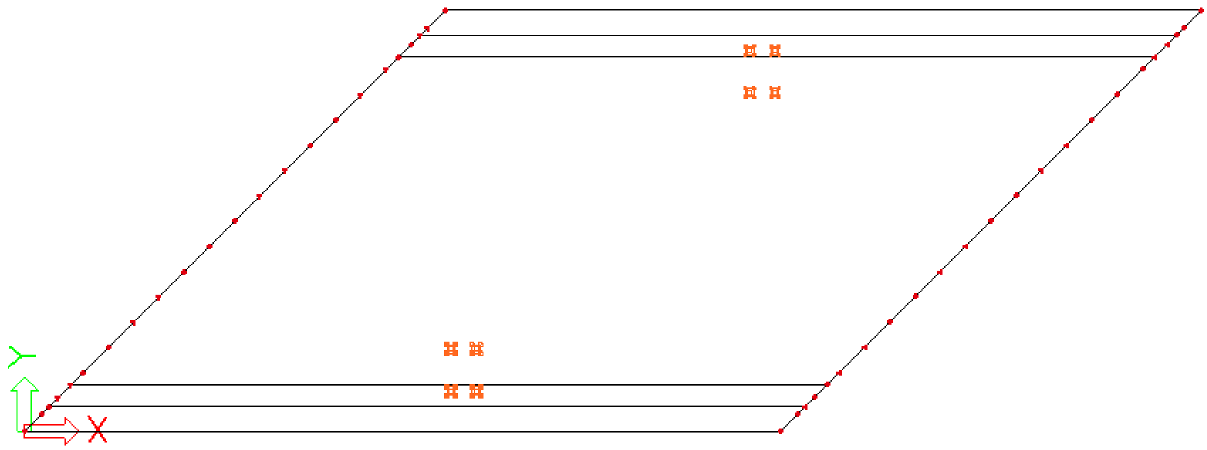

Figure B-4 Applied axle loads for maximum negative moments (with corresponding negative working lane loads)

From this load case follows governing moments, presented in Table B-2.

Position	Straight bridge [kNm]	Skew bridge [kNm]	Deviation [%]
Deck positive	+28.0	+31.7	+13.21
Deck negative	-16.5	-12.5	-24.24
Deck corner negative	-35.6	-46.8	+31.46

Table B-2 Comparison transversal moment

To get insight, the distribution of the transverse bending moment is visualized in Figure B-5, Figure B-6 and Figure B-7 and Figure B-8 for both the straight and skew bridge. The color range was set the same to be able to compare the colours.

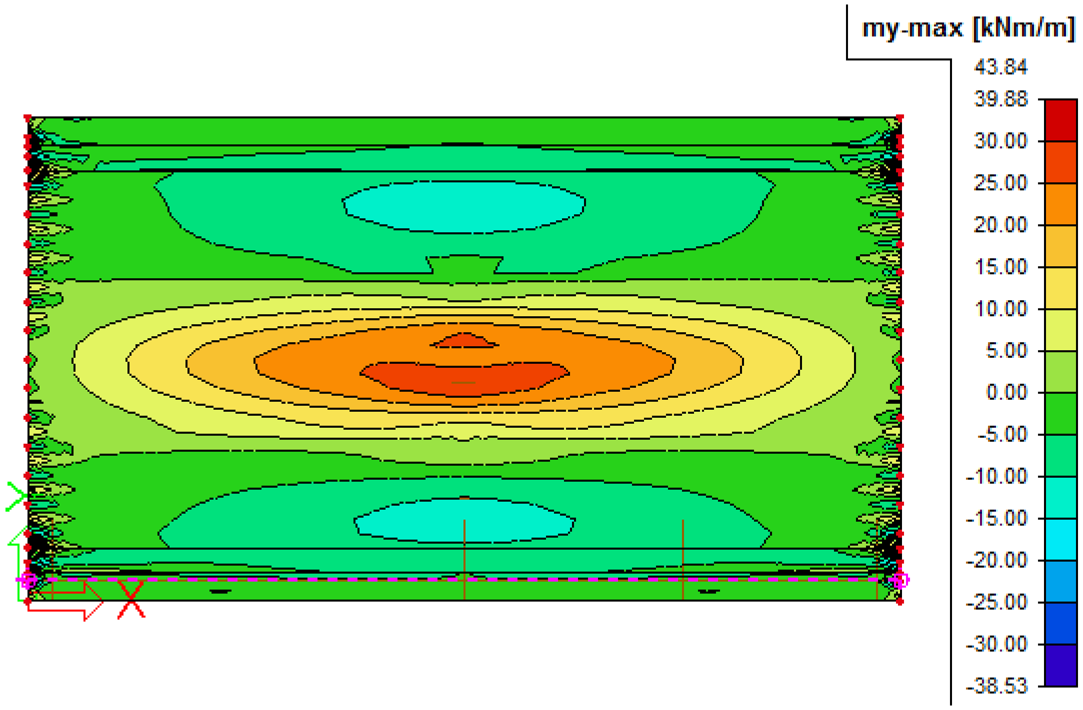

Figure B-5 Positive moments in deck straight bridge

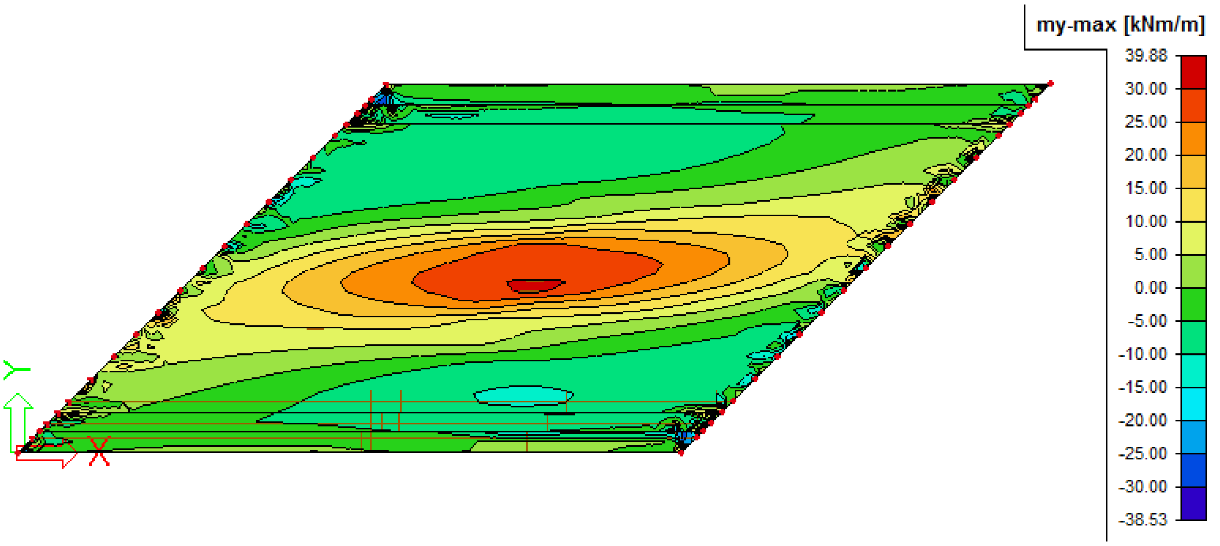

Figure B-6 Positive moments in deck skew bridge

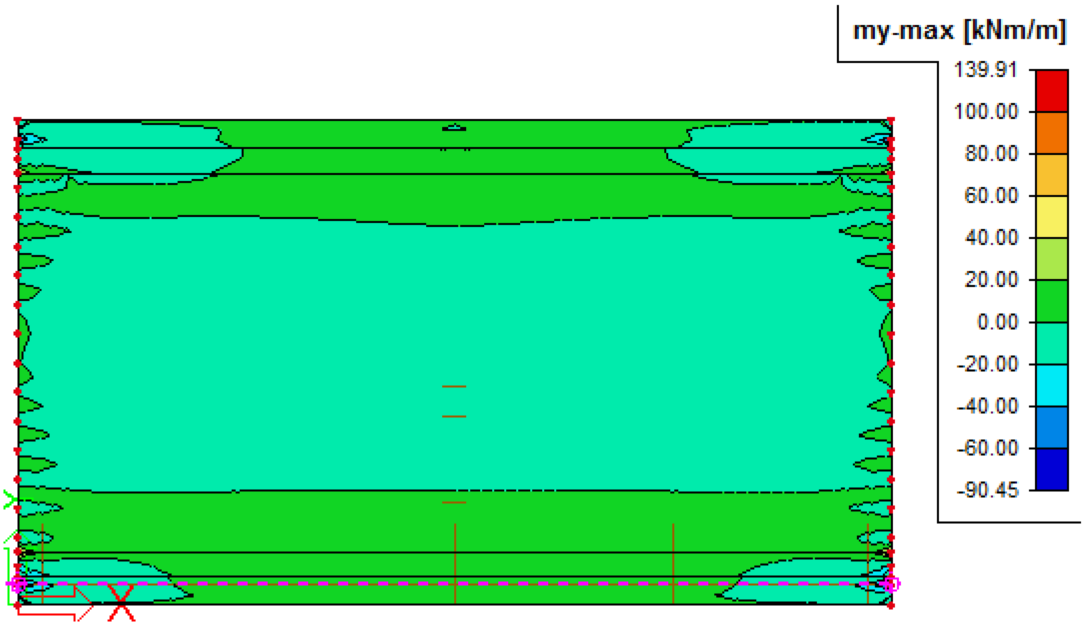

Figure B-7 Negative moments in deck straight bridge

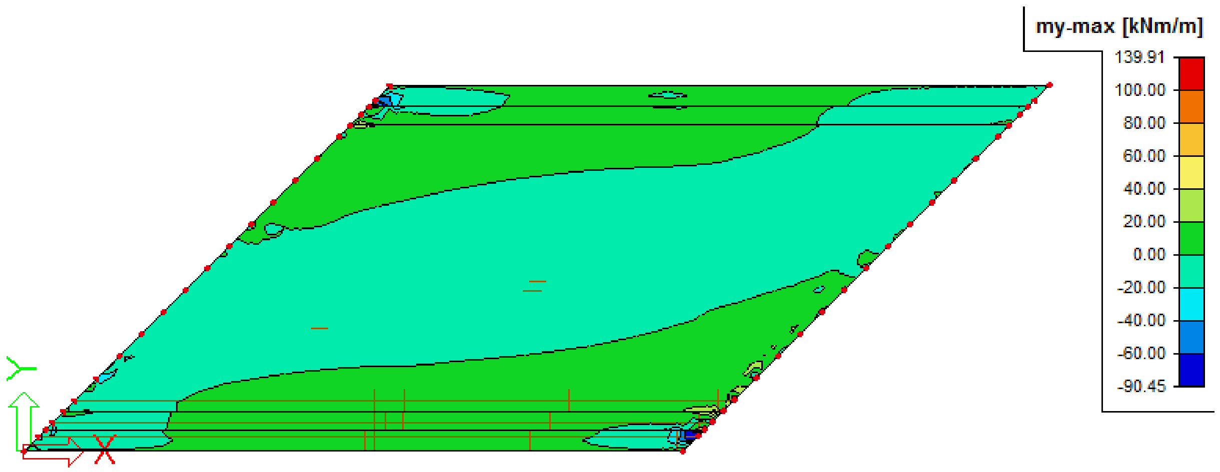

Figure B-8 Negative moments in deck skew bridge

Positive moments in deck
The positive moment in the deck is higher for the skew bridge (Table B-2).

Minalu gets the same result, also an increase of transversal moments, but only of 7.4 %. Minalu compared some angles of skewness and founds that with angles larger than 45 degree the moments increase much more compared to a straight bridge. It is clear that the load transfer will be more direct to the obtuse corners dependent on the skewness, logically the transverse moments increase in that case.

Negative moments in deck and corners
The negative moment in the deck is lower for the skew bridge in the middle but higher in the corner of the bridge, Table B-2. That the negative moments decrease for the skew one is remarkable. A calculation of a skew bridge based on a straight bridge model consequently will give an underestimation of the negative moments. The negative moments at the obtuse corners enhance a lot. A reason for this could be: When the obtuse corner attracts more load it attracts more negative moments.

Minalu did not analyse the occurring negative moments in the deck, so no comparison can be made with his results.

Relation between torsion and moments in deck
Interesting is the question: why is are there differences in the moments in the deck between the skw and straight bridge? For that reason the distribution of the torsion moments is visualised in Figure B-9 and Figure B-10.

Some remarkable points:

- In the straight bridge the positive and negative torsion moments are bounded in the quadrants. In the skew one the negative quadrants are joining together.
- For the straight bridge the maxima of the torsion moments are +26.09/ -26.10 kNm. For the skew one they are +69.1/ -82.7 kNm.
- The green color between -10 and -20 kNm is occurring more in the skew bridge: more torsion.

From this it can be concluded that the transversal bending moment in the middle of the deck is decreasing because the torsion moments are bearing a larger part of the load.

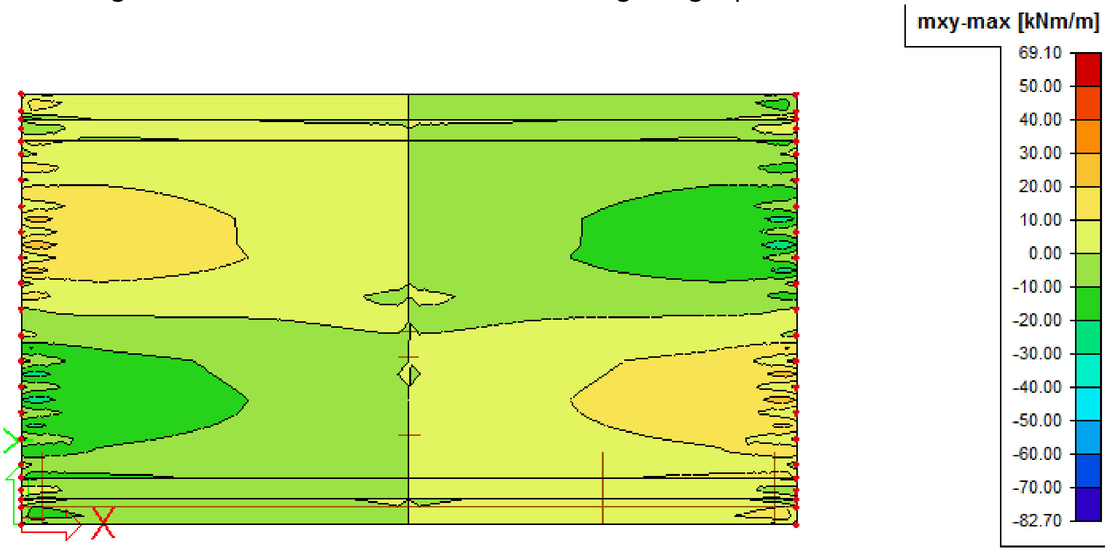

Figure B-9 Torsion moments occurring together with positive bending moments in deck for straight bridge

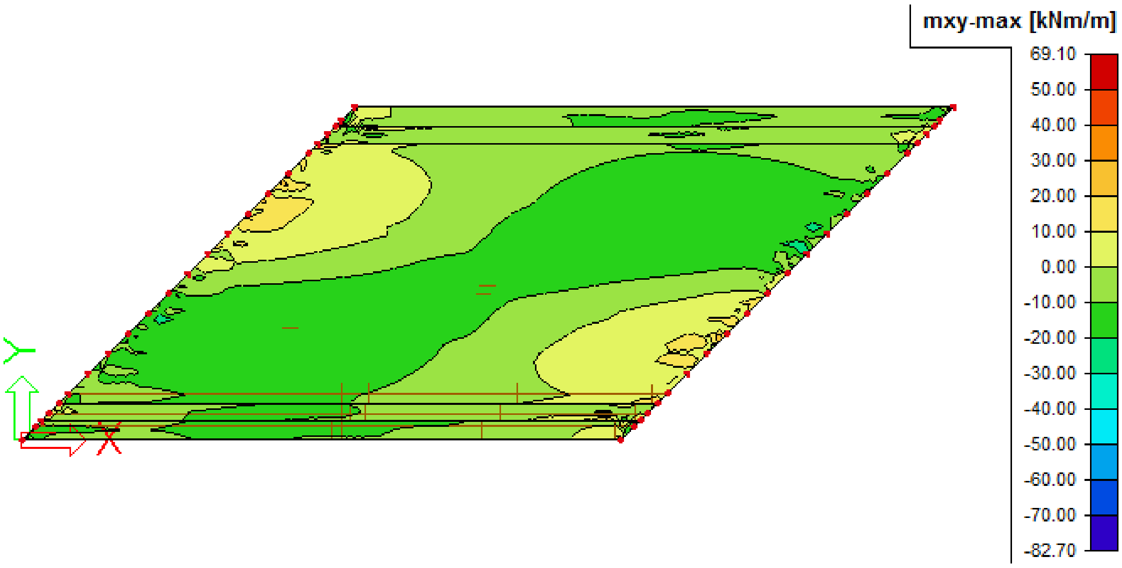

Figure B-10 Torsion moments occurring together with positive bending moments in deck for skew bridge

Torsion and Shear force in girders

Intended comparison

- First it will be investigated if it was a save assumption to use the practical models and neglect the models found by Minalu.
- After that differences between the skew and straight bridge will be analysed.

Load models

The load models used for the determination of the shear and torsion reinforcement are presented in Figure B-11 and Figure B-12. In practice train loads are used to model this load cases in one run.

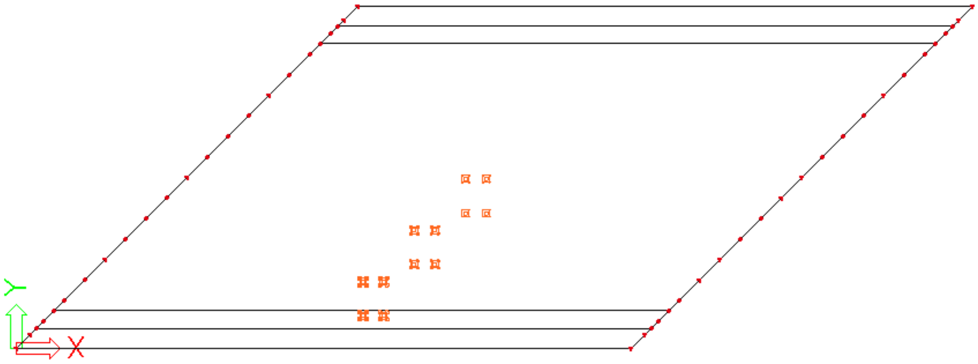

Figure B-11 Case 1: Loads for maximum longitudinal moment and shear (with corresponding negative working lane loads)

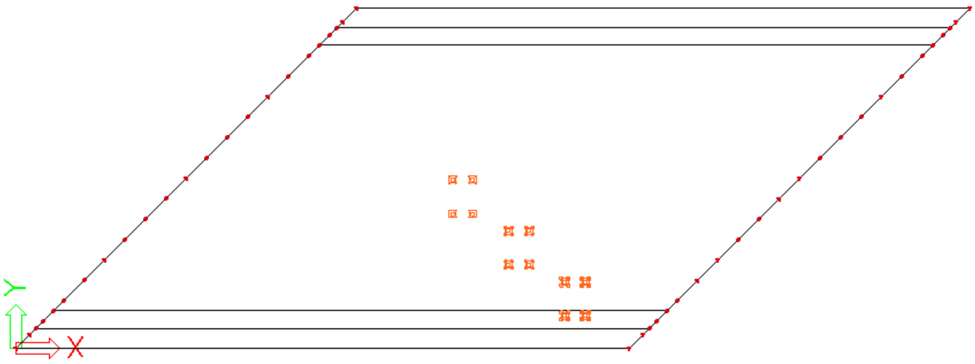

Figure B-12 Case 2: Loads for maximum shear and torsion (with corresponding negative working lane loads)

Minalu developed load configurations for maximum torsional moment in the first ZIP girder presented in Figure B-13 and Figure B-14. That configuration is not used to calculate the reinforcement in this report because in practice it is not used too.

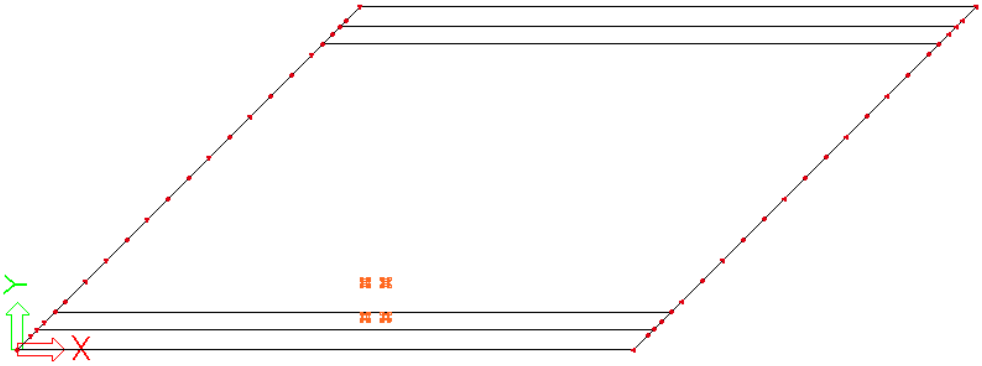

Figure B-13 Case 3: Load case for maximum negative torsional moment (with corresponding negative working lane loads)

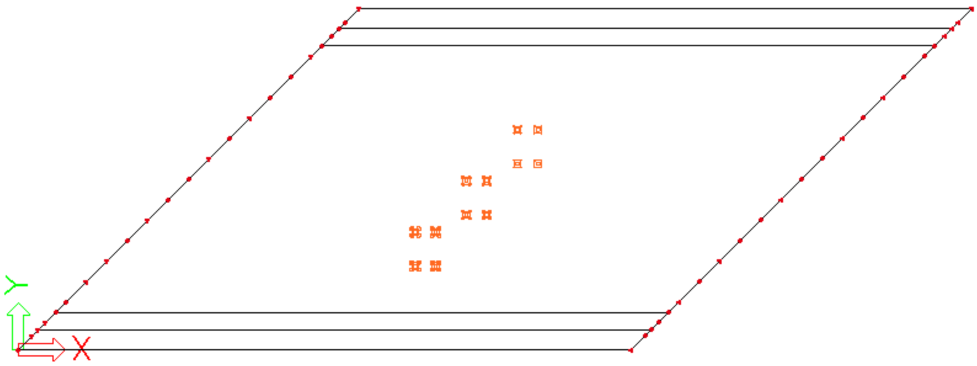

Figure B-14 Case 4: Load case for maximum negative torsional moment (with corresponding positive working lane loads)

Output for straight bridge

The four presented models give output which is presented in Table B-3 (shear force) and Table B-4 (torsion).

Remarks:

- The used values in the calculation, following from load case 1 and 2 are marked grey. The calculation is based on three points at end, quarter and half of span. So the point 0.88 L is not used but only added for comparison.
- Highest values, following from all loud cases, are marked bold and underlined.
- The values of the ZIP and first ZIP are all compared, the maximum is taken and applied to one design ZIP girder.

Girder		Straight bridge [kN]			
		Case 1	Case 2	Case 3	Case 4
ZIP	0	313,3	252,7	265,1	179,4
	0.5L	0,0	**<u>18,2</u>**	0,0	0,0
	0.75L	**<u>204,1</u>**	103,1	170,8	118,2
	0.88L	**<u>255,5</u>**	185,4	214,3	156,2
	L	313,3	**<u>418,0</u>**	265,1	179,4
1st ZIP	0	268,8	215,3	237,7	143,8
	0.5L	0,0	12,1	0,0	0,0
	0.75L	182,1	104,9	162,7	89,7
	0.88L	250,2	146,4	228,0	128,5
	L	268,8	342,3	237,7	143,8
TRA	0	284,6	233,5	302,4	116,1
	0.5L	0,0	**<u>5,6</u>**	0,0	0,0
	0.75L	**<u>148,2</u>**	100,3	151,7	47,8
	0.88L	198,7	162,2	**<u>200,7</u>**	77,4
	L	284,6	265,1	**<u>302,4</u>**	116,1

Table B-3 Shear forces from Scia in straight bridge

Girder		Straight bridge [kNm]			
		Case 1	Case 2	Case 3	Case 4
ZIP	0	10,4	9,3	36,7	-35,9
	0.5L	0,0	-2,6	0,0	0,0
	0.75L	-10,6	-9,5	**<u>-30,5</u>**	25,7
	0.88L	-15,3	-8,2	**<u>-40,6</u>**	32,2
	L	-10,4	0,6	-36,7	35,9
1st ZIP	0	23,0	21,2	47,0	-21,7
	0.5L	0,0	**<u>-2,8</u>**	0,0	0,0
	0.75L	-6,0	-9,4	-23,4	18,7
	0.88L	-12,7	-10,5	-35,8	21,5
	L	-23,0	-16,1	**<u>-47,0</u>**	21,7
TRA	0	-9,9	-6,6	10,9	-28,5
	0.5L	0,0	**<u>-3,6</u>**	0,0	0,0
	0.75L	-4,3	-12,2	**<u>-25,5</u>**	22,1
	0.88L	-3,4	-4,5	**<u>-29,1</u>**	27,6
	L	9,9	18,0	-10,9	**<u>28,5</u>**

Table B-4 Torsion moments in straight bridge

Applied forces on straight bridge

From Table B-3 and Table B-4 the maximum forces can be extracted and used in the calculation. This is done with the standard method of Spanbeton presented in Table B-5 and Table B-6.

Remarks:

- The maximum forces are split up in to parts. That is done in relation to the fatigue calculation. One example how to find the relation between the ‘output’ and ‘applied forces’ is: Maximum shear in ZIP at location L, output gives 418 kN, that is presented as 82,3 + 335,7 kNm.
- The moments due to own weight of the girders and deck is simply calculated with $1/8*q*L^2$
- The dead loads already give torsion in the girders ($T_{rep;rust}$), only when the live loads give higher torsion the differences are added ($T_{rep;nut}$).

Cut at:	$V_{rep;eg;pref}$ [kN]	$V_{rep;eg;dl}$ [kN]	$V_{rep;rust}$ [kN]	$V_{rep;nut}$ [kN]	$T_{rep;rust}$ [kNm]	$T_{rep;nut}$ [kNm]	V_d [kN]	T_d [kNm]
γ =	1,35	1,35	1,35	1,35	1,35	1,35	-	-
Support	251,5	127,1	82,3	335,7	28,8	0	1075	39
1/4 L_T	125,8	63,5	52,9	151,2	13,7	0	531	18
1/2 L_T	0	0	0	18,2	0	2,8	25	4

Table B-5 Applied loads for ZIP girders

Cut at:	$V_{rep;eg;pref}$ [kN]	$V_{rep;eg;dl}$ [kN]	$V_{rep;rust}$ [kN]	$V_{rep;nut}$ [kN]	$T_{rep;rust}$ [kNm]	$T_{rep;nut}$ [kNm]	V_d [kN]	T_d [kNm]
γ =	1,35	1,35	1,35	1,35	1,35	1,35	-	-
Support	247,1	134,1	146,4	138,2	10,7	7,3	899	24
1/4 L_T	123,6	37,1	51,7	96,5	17,8	0	417	24
1/2 L_T	0	0	0	5,6	0	3,6	8	5

Table B-6 Applied loads for TRA girders

Evaluation used load models for straight bridge

The reinforcement from the four load cases will be compared with the calculated reinforcement from the calculation (based on load case 1 and 2).

Two cases will be compared:

1. Maximum shear force with occurring torsion at same time, Table B-7.
2. Maximum torsion with occurring shear force at same time, Table B-8.

Girder		Straight bridge [kN]		Check	Needed area reinforcement [mm]	
		Shear force	Torsion		Case 1 and 2	Max shear
ZIP	0.5L	18,2	-2,8	OK		
	0.75L	204,1	-10,6	OK		
	0.88L	255,5	-15,3	OK		
	L	418,0	-16,6	OK		
TRA	0.5L	5,6	-3,6	OK		
	0.75L	148,2	-4,3	OK		
	0.88L	200,7	-29,1	?	0	0
	L	302,4	-10,9	?	1222	**1261**

Table B-7 Maximum shear force with occurring torsion, maximum from all cases

Girder		Straight bridge [kNm]		Check	Needed area reinforcement [mm]	
		Shear force	Torsion		Case 1 and 2	Max torsion
ZIP	0.5L	18,2	-2,8	OK		
	0.75L	170,8	-30,5	?	0	0
	0.88L	214,3	-40,6	?	0	0
	L	265.1	-47,0	?	1457	1160
TRA	0.5L	5,6	-3,6	OK		
	0.75L	151,7	-25,5	?	0	0
	0.88L	200,7	-29,1	?	0	0
	L	116,1	28,5	?	1222	828

Table B-8 Maximum torsion with occurring shear force, maximum from all cases

From Table B-7 it appears that one time load case 3 needs more reinforcement, but this is only 3 % more. The applied reinforcement will be always a bit more, so this will not give differences in practice. So for the straight bridge it is sufficient to use only load case 1 and 2.

Output for skew bridge

The four presented models give output which is presented in Table B-9 (shear force) and Table B-10 (torsion).

Remarks:

- The used values in the calculation, following from load case 1 and 2 are marked grey. The calculation is based on three points at end, quarter and half of span. So the point 0.88 L is not used but only added for comparison.
- Highest values, following from all loud cases, are marked bold and underlined.
- The values of the ZIP and first ZIP are all compared, the maximum is taken and applied to one design ZIP girder.

Girder		Straight bridge [kN]			
		Case 1	Case 2	Case 3	Case 4
ZIP	0	295,1	253,4	271,8	144,0
	0.5L	2,5	31,6	12,6	14,3
	0.75L	**205,4**	91,4	176,0	112,1
	0.88L	241,2	**291,2**	191,6	160,9
	L	281,6	**371,8**	212,2	203,9
1st ZIP	0	256,0	221,3	241,3	132,0
	0.5L	**98,9**	26,7	96,3	5,3
	0.75L	184,2	93,8	168,5	86,4
	0.88L	265,0	281,3	243,4	133,3
	L	249,6	330,2	203,4	158,5
TRA	0	292,5	254,5	289,2	162,7
	0.5L	10,7	5,9	**18,6**	15,2
	0.75L	**162,0**	114,8	158,9	63,0
	0.88L	222,3	194,6	**224,1**	85,3
	L	308,5	296,4	**328,1**	109,6

Table B-9 Shear forces from Scia in skew bridge

Girder		Straight bridge [kNm]			
		Case 1	Case 2	Case 3	Case 4
ZIP	0	12,3	10,8	29,6	-24,6
	0.5L	-33,9	-32,0	-25,1	-26,6
	0.75L	-39,5	-34,8	**-52,7**	3,9
	0.88L	-33,9	-25,7	-54,9	18,8
	L	-19,2	-7,8	-43,0	32,2
1st ZIP	0	16,3	13,5	33,7	-8,0
	0.5L	**-34,3**	-31,6	-26,8	-23,6
	0.75L	-35,6	-35,2	-47,4	-0,7
	0.88L	-37,8	-28,3	**-59,3**	10,9
	L	-44,2	-27,7	**-71,5**	12,5
TRA	0	-21,2	-17,6	-8,1	-29,1
	0.5L	**-47,1**	-41,6	-36,0	-32,1
	0.75L	-43,7	-49,1	**-56,3**	-6,2
	0.88L	-36,6	-30,4	**-59,8**	8,6
	L	-16,9	-0,9	**-41,3**	27,0

Table B-10 Torsion moments in skew bridge

Applied forces on skew bridge

From Table B-9 and Table B-10 the maximum forces can be extracted and used in the calculation. This is done with the standard method of Spanbeton presented in Table B-11 and Table B-12.

Remarks:

- The maximum forces are split up in to parts. That is done in relation to the fatigue calculation. One example how to find the relation between the 'output' and 'applied forces' is: Maximum shear in ZIP at location L, output gives 371,8 kN, that is presented as 101,8 + 270 kNm.
- The moments due to own weight of the girders and deck is simply calculated with $1/8*q*L^2$
- The dead loads already give torsion in the girders ($T_{rep;rust}$), only when the live loads give higher torsion the differences are added ($T_{rep;nut}$).

Cut at: $\gamma =$	$V_{rep;eq;pref}$ [kN] 1,35	$V_{rep;eq;dl}$ [kN] 1,35	$V_{rep;rust}$ [kN] 1,35	$V_{rep;nut}$ [kN] 1,35	$T_{rep;rust}$ [kNm] 1,35	$T_{rep;nut}$ [kNm] 1,35	V_d [kN] -	T_d [kNm] -
Support	251,5	127,1	101,8	270	37,1	7,1	251,5	127,1
1/4 L_T	125,8	63,5	88,3	117,1	22,3	17,2	125,8	63,5
1/2 L_T	0	0	4,9	94	9,2	25,1	0	0

Table B-11 Applied loads for ZIP girders

Cut at: $\gamma =$	$V_{rep;eq;pref}$ [kN] 1,35	$V_{rep;eq;dl}$ [kN] 1,35	$V_{rep;rust}$ [kN] 1,35	$V_{rep;nut}$ [kN] 1,35	$T_{rep;rust}$ [kNm] 1,35	$T_{rep;nut}$ [kNm] 1,35	V_d [kN] -	T_d [kNm] -
Support	247,1	134,1	154	154,5	28,1	0	931	38
1/4 L_T	123,6	37,1	55	107	28,9	20,2	436	66
1/2 L_T	0	0	0,9	9,8	10,3	36,8	14	64

Table B-12 Applied loads for TRA girders

Evaluation used load models for skew bridge

The reinforcement from the four load cases will be compared with the calculated reinforcement from the calculation (based on load case 1 and 2).

Two cases will be compared:

1. Maximum shear force with occurring torsion at same time, Table B-13.
2. Maximum torsion with occurring shear force at same time, Table B-14.

Girder		Skew bridge [kN]		Check	Needed area reinforcement [mm]	
		Shear force	Torsion		Case 1 and 2	Max shear
ZIP	0.5L	98,9	-34,3	OK		
	0.75L	205,4	-39,5	OK		
	0.88L	291,2	-28,3	OK		
	L	371,8	-27,7	OK		
TRA	0.5L	18,6	-36,0	?	0	0
	0.75L	162,0	-43,7	OK		
	0.88L	224,1	-59,8	?	0	0
	L	328,1	-41,3	?	1382	**1560**

Table B-13 Maximum shear force with occurring torsion, maximum from all cases

Girder		Skew bridge [kNm]		Check	Needed area reinforcement [mm]	
		Shear force	Torsion		Case 1 and 2	Max torsion
ZIP	0.5L	89,9	-34,3	OK		
	0.75L	176,0	-52,7	?	0	0
	0.88L	243,4	-59,3	?	0	0
	L	241,3	-71,5	?	1445	1290
TRA	0.5L	10,7	-47,1	OK		
	0.75L	158,9	-56,3	?	0	0
	0.88L	224,1	-59,8	?	0	0
	L	328,1	-41,3	?	1382	**1560**

Table B-14 Maximum torsion with occurring shear force, maximum from all cases

From Table B-13 it appears that one time the TRA needs more reinforcement for load case 3, this is 13 % more. This is available due to the fatigue calculation that is governing, so it will not give other reinforcement. However, it is a serious difference.

Comparison with results of Minalu

Minalu searches the largest torsional moments in the first ZIP girder. He didn’t look to the shear forces at all, so the interaction between torsion and shear wasn’t investigated. Furthermore he takes an cut along the length of the beam, but didn’t apply averaging over the width of the girder. Another difference is that he models the end diaphragm beam, that was not done in this calculation. Comparison with his values is therefore not possible.

Comparison straight and skew bridge

The results for the straight and skew bridge are analysed in detail. Now a comparison between the two bridges is made.

Two effects are visible:

1. In the skew bridge the shear force is normally higher.
2. In the skew bridge also the torsion moments are higher.

The effects are visualized in Table B-15, Table B-16, Figure B-15 and Figure B-16. It follows clearly that there is much more torsion in a the skew bridge compared with the straight one.

Girder		Straight	Skew	Deviation [%]
ZIP	0.5L	18,2	98,9	442,9
	0.75L	204,1	205,4	0,6
	L	418,0	371,8	-11,1
TRA	0.5L	5,6	10,7	91,1
	0.75L	148,2	162,0	9,3
	L	284,6	308,5	8,4

Table B-15 Comparison shear force in straight and skew bridge

Girder		Straight	Skew	Deviation [%]
ZIP	0.5L	-2,8	-34,3	1125,0
	0.75L	-10,6	-39.5	178,3
	L	-23,0	-44,2	92,2
TRA	0.5L	-3,6	-47,1	1208,3
	0.75L	-12,2	-49,1	302,5
	L	18,0	-16,9	-6,1

Table B-16 Comparison torsion moment in straight and skew bridge

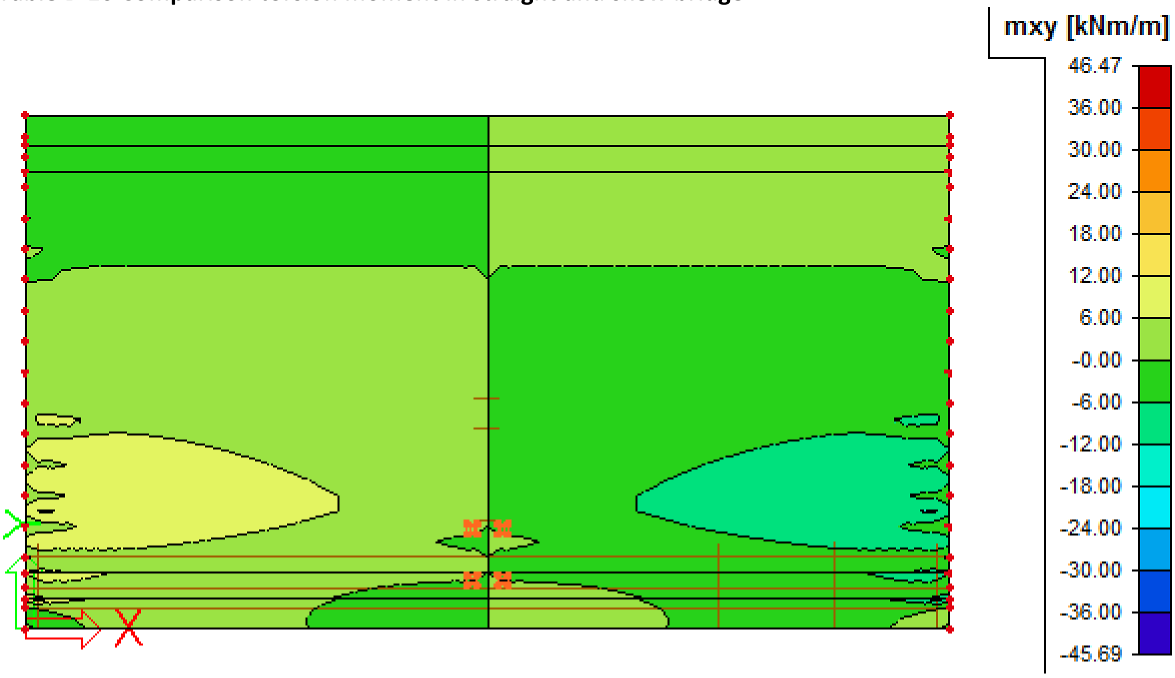

Figure B-15 Torsion in straight bridge due to load case 2

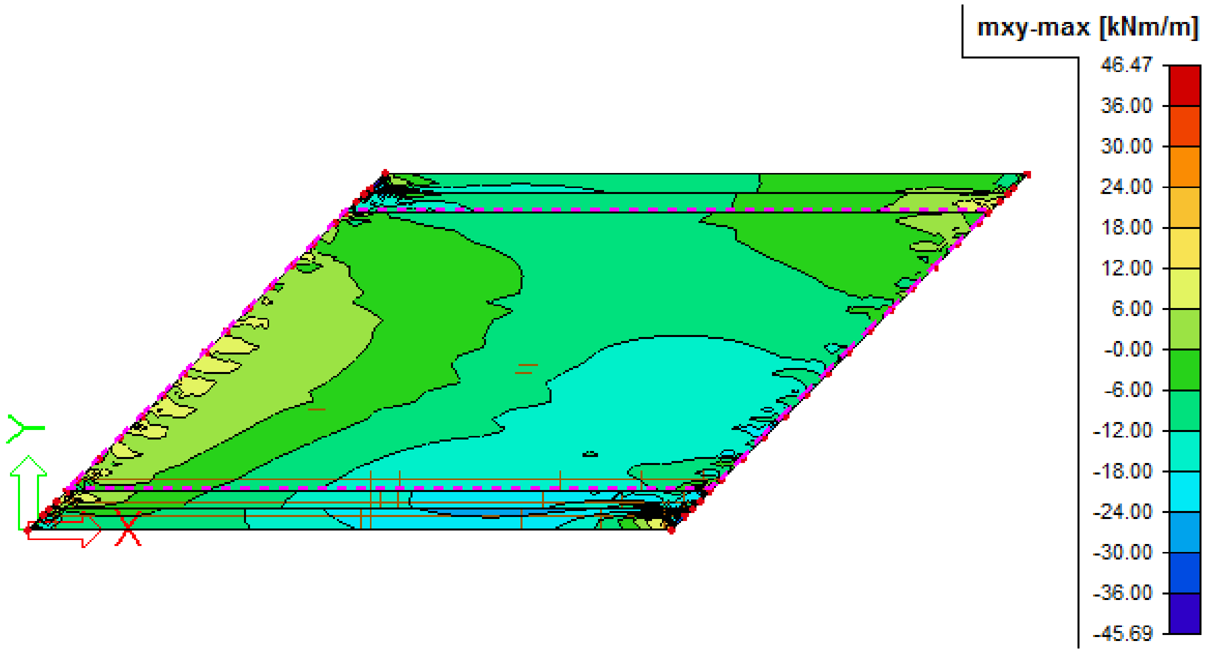

Figure B-16 Torsion in skew bridge due to load case 2

Answer to intended comparison

- The developed load cases by Minalu have no effect on the reinforcement of the ZIP girders. For the TRA sometimes load case 3 (Figure B-13) will give the most severe combination. A practical rule would be to check the TRA for load case 3. On the other hand, due to the fatigue rules no problems will occur because that is the governing phenomena.
- In a skew bridge occurs higher torsion moments and shear forces.

Issues from analysis

- When the positive moments in the deck of a skew bridge are based on a straight bridge model an underestimation of that moment can occur.
- The torsional moments reduces the negative moments in the middle of the deck. When these torsional moments are neglected higher negative moments in the deck are found. Consequently there will be an underestimation of the positive moments.
- Is it true that heavy negative moments occur at the corner of the deck in the orthotropic plate model?[19]

[19] Minalu, Kassuhun K. (2010), *Finite element modelling of skew slab-girder bridges.* Page 68.

C. Determination bond length following the Eurocode

Inleidingslengte voorspanning l_{pt2} = 1139 mm NEN-EN1992-1-1:2005 (8.18)

$l_{pt2} = 1{,}2 \cdot l_{pt}$

Bepalen inleidingslengte:

$f_{bpt} = \eta_{p1} \cdot \eta_1 \cdot f_{ctd}(t)$		$l_{pt} = \alpha_1 \alpha_2 \phi \sigma_{pm0} / f_{bpt}$	
η_{p1} =	3,2	σ_{pm0} =	1222 N/mm^2
η_1 =	1,0	α_1 =	1,25
$f_{ctd}(t)$ =	1,50 N/mm^2	α_2 =	0,19
		ϕ =	15,7 mm
$\Rightarrow f_{bpt}$ =	4,8 N/mm^2	$\Rightarrow l_{pt}$ =	949 mm

(2) Voorspankanalen voor nagespannen elementen behoren in het algemeen niet te zijn gebundeld met uitzondering van het geval van twee voorspankanalen die verticaal boven elkaar geplaatst zijn.

(3) De minimale vrije afstand tussen voorspankanalen behoort in overeenstemming te zijn met hetgeen is getoond in figuur 8.15.

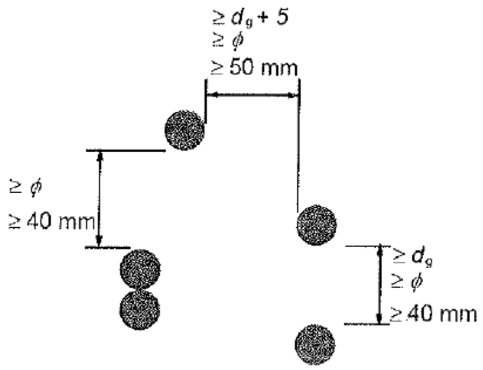

OPMERKING ϕ is de diameter van voorspankanalen voor nagerekt staal en d_g is de maximale korrelafmeting.

Figuur 8.15 — Minimale vrije afstand tussen voorspankanalen

8.10.2 Verankering van voorspanelementen met voorgerekt staal

8.10.2.1 Algemeen

(1) In verankeringsgebieden van voorspanelementen met voorgerekt staal behoren de volgende lengteparameterss te zijn beschouwd, zie figuur 8.16:

a) De overdrachtslengte l_{pt}, waarover de voorspankracht (P_0) volledig is overgedragen op het beton; zie 8.10.2.2 (2);

b) De spreidingslengte l_{disp} waarover de betonspanning geleidelijk is gespreid tot een lineaire verdeling over de betondoorsnede, zie 8.10.2.2 (4);

c) De verankeringslengte l_{bpd}, waarover de spankracht F_{pd} in de uiterste grenstoestand volledig is verankerd in het beton; zie 8.10.2.3 (4) en (5).

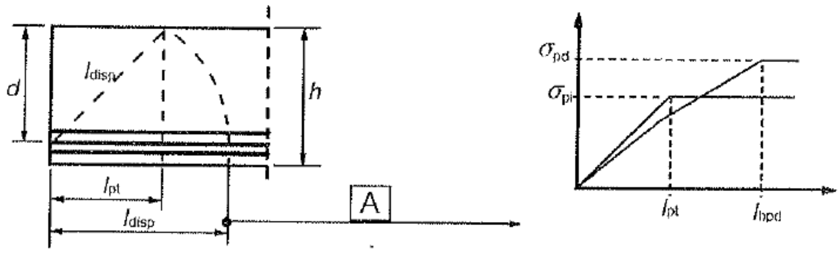

Verklaring

A lineaire spanningsverdeling in de dwarsdoorsnede van een element

Figuur 8.16 — Overdracht van voorspanning in elementen met voorgerekt staal; lengteparameters

8.10.2.2 Overdracht van de voorspanning

(1) Bij het aflaten van de spanelementen mag zijn aangenomen dat de voorspanning op het beton is overgedragen door een constante aanhechtspanning f_{bpt}, waarin:

$$f_{bpt} = \eta_{p1}\, \eta_1\, f_{ctd}(t) \tag{8.15}$$

waarin:

η_{p1} is een coëfficiënt die rekening houdt met het type spanelement en de aanhechtingssituatie bij het aflaten;
η_{p1} = 2,7 voor gedeukte draden;
η_{p1} = 3,2 voor 3- en 7-draads strengen;

η_1 = 1,0 voor goede aanhechtingsomstandigheden (zie 8.4.2);
= 0,7 in andere gevallen, tenzij een hogere waarde kan zijn gerechtvaardigd met betrekking tot speciale omstandigheden bij de uitvoering;

$f_{ctd}(t)$ is de rekenwaarde van de treksterkte op het tijdstip van aflaten;
$f_{ctd}(t)$ = $\alpha_{ct} \cdot 0{,}7 \cdot f_{ctm}(t) / \gamma_c$ (zie ook 3.1.2 (8) en 3.1.6 (2)P).
$\alpha_{ct} = 1{,}0$

OPMERKING Waarden van η_{p1} voor andere dan hierboven gegeven typen spanelementen kunnen zijn gebruikt op grond van een Europese Technische Goedkeuring.

(2) De basiswaarde van de overdrachtslengte l_{pt}, is gegeven door:

$$l_{pt} = \alpha_1\, \alpha_2\, \phi\, \sigma_{pm0}/f_{bpt} \tag{8.16}$$

waarin:

α_1 = 1,0 voor geleidelijk aflaten;
= 1,25 voor plotseling aflaten;

α_2 = 0,25 voor spanelementen met cirkelvormige doorsnede;
= 0,19 voor 3- en 7-draads strengen;

ϕ is de nominale diameter van het spanelement;

σ_{pm0} is de spanning in het spanelement juist na het aflaten.

(3) Voor de rekenwaarde van de overdrachtslengte behoort de meest ongunstige van twee waarden te zijn genomen, afhankelijk van de ontwerpsituatie:

$$l_{pt1} = 0{,}8\, l_{pt} \tag{8.17}$$

of

$$l_{pt2} = 1{,}2\, l_{pt} \tag{8.18}$$

OPMERKING In het algemeen wordt de lagere waarde gebruikt voor toetsing van lokale spanningen bij het aflaten en de hogere waarde voor de uiterste grenstoestanden (dwarskracht, verankering enz.).

(4) Aangenomen mag zijn dat de betonspanning buiten de spreidingslengte een lineaire verdeling heeft, zie figuur 8.17:

$$l_{disp} = \sqrt{l_{pt}^2 + d^2} \tag{8.19}$$

(5) Een alternatieve opbouw van de voorspanning mag zijn aangenomen als dit afdoende kan zijn gerechtvaardigd en als de overdrachtslengte overeenkomstig is aangepast.

8.10.2.3 Verankering van de trekkracht in de uiterste grenstoestand

(1) De verankering van voorspanelementen behoort te zijn gecontroleerd in doorsneden waarin de betontrekspanning $f_{ctk,0,05}$ overschrijdt. De kracht in het voorspanelement behoort te zijn berekend voor een gescheurde doorsnede inclusief het effect van dwarskracht volgens 6.2.3 (6); zie ook 9.2.1.3. Indien de betontrekspanning kleiner is dan $f_{ctk,0,05}$, is controle van de verankering niet nodig.

(2) De aanhechtsterkte voor verankering in de uiterste grenstoestand is:

$$f_{bpd} = \eta_{p2}\, \eta_1\, f_{ctd} \tag{8.20}$$

waarin:

η_{p2} is een coëfficiënt die rekening houdt met het type spanelement en de aanhechtingssituatie bij de verankering;
η_{p2} = 1,4 voor gedeukte draden of
η_{p2} = 1,2 voor 7-draads strengen;

η_1 is zoals gedefinieerd in 8.10.2.2 (1).

OPMERKING Waarden van η_{p2} voor andere dan de hierboven gegeven types voorspanelementen kunnen zijn gebruikt op grond van een Europese Technische Goedkeuring.

(3) Ten gevolge van toenemende brosheid bij beton met hogere sterkte behoort $f_{ctk,0,05}$ hierbij te zijn beperkt tot de waarde voor C60/75, tenzij kan zijn getoetst dat de gemiddelde aanhechtsterkte uitstijgt boven deze grens.

(4) De totale verankeringslengte voor het verankeren van een voorspanelement met spanning σ_{pd} is:

$$l_{bpd} = l_{pt2} + \alpha_2 \phi\, (\sigma_{pd} - \sigma_{pm\infty})/f_{bpd} \tag{8.21}$$

waarin:

l_{pt2} is de grootste rekenwaarde van de overdrachtslengte, zie 8.10.2.2 (3);
α_2 als gedefinieerd in 8.10.2.2 (2);
σ_{pd} is de spanning in het spanelement overeenkomend met de in (1) beschreven kracht;
$\sigma_{pm\infty}$ is de voorspanning na alle verliezen.

(5) Spanningen in het voorspanstaal in het verankeringsgebied zijn geïllustreerd in figuur 8.17.

NEN-EN 1992-1-1:2005

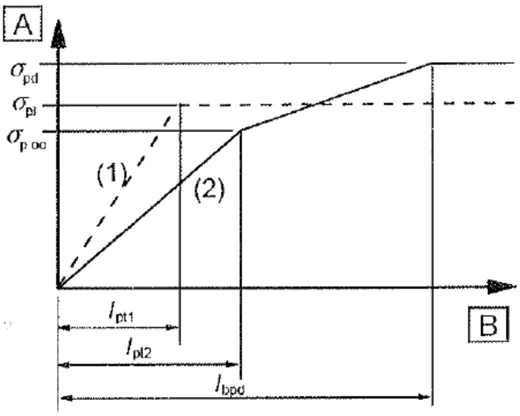

Verklaring

A spanning in het voorspanstaal
B afstand vanaf het uiteinde

Figuur 8.17 — Spanningen in het verankerinsgebied van elementen met voorgerekt staal: (1) bij het aflaten van de spanelementen, (2) in de uiterste grenstoestand

(6) Bij combinaties van gewone wapening en voorspanwapening mogen de verankeringscapaciteiten van beide bij elkaar zijn opgeteld.

8.10.3 Verankeringszones van elementen voorgespannen met nagerekt staal

(1) Het berekenen van verankeringszones behoort in overeenstemming te zijn met de toepassingsregels in deze paragraaf en die in 6.5.3

(2) Bij het beschouwen van de effecten van de voorspanning als een geconcentreerde kracht op de verankeringszone behoort de rekenwaarde van de voorspanelementen in overeenstemming te zijn met 2.4.2.2 (3) en behoort de lagere karakteristieke treksterkte van het beton te zijn gebruikt.

(3) De oplegdruk achter verankeringsplaten behoort te zijn gecontroleerd in overeenstemming met de van toepassing zijnde Europese Technische Goedkeuring.

(4) Trekkrachten ten gevolge van geconcentreerde krachten behoren te zijn bepaald met een staafwerkmodel of een andere geschikte methode (zie 6.5). Bij het detailleren van de wapening behoort te zijn aangenomen dat de staalspanning gelijk is aan de rekenwaarde van de sterkte. Als de spanning in deze wapening is beperkt tot 300 MPa, is controle van de scheurwijdte niet nodig.

D. Derivation of force distribution in ZIP girder

The force distribution from the prestressing is derived, including the effects in the bond zone.

Geometry

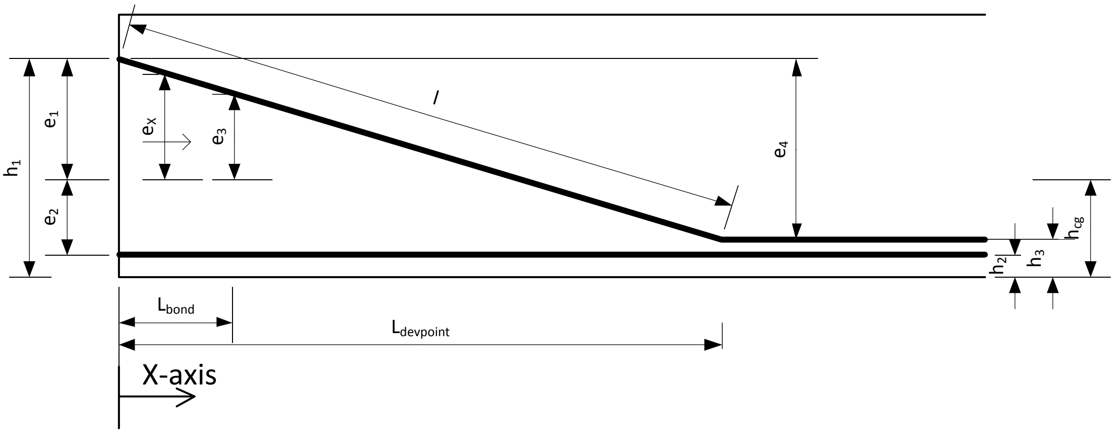

$$l = \sqrt{L_{devpoint}^2 + e_4^2}$$
$$e_1 = h_1 - h_{cg}$$
$$e_2 = h_{cg} - h_2$$
$$e_3 = \frac{(L_{devpoint} - L_{bond})}{L_{devpoint}} \cdot e_4 + h_3 - h_{cg}$$
$$e_4 = h_1 - h_3$$
$$e(x) = e_1 - \frac{e_1 - e_3}{L_{bond}} \cdot x \; voor \; 0 < x < L_{bond}$$

Forces

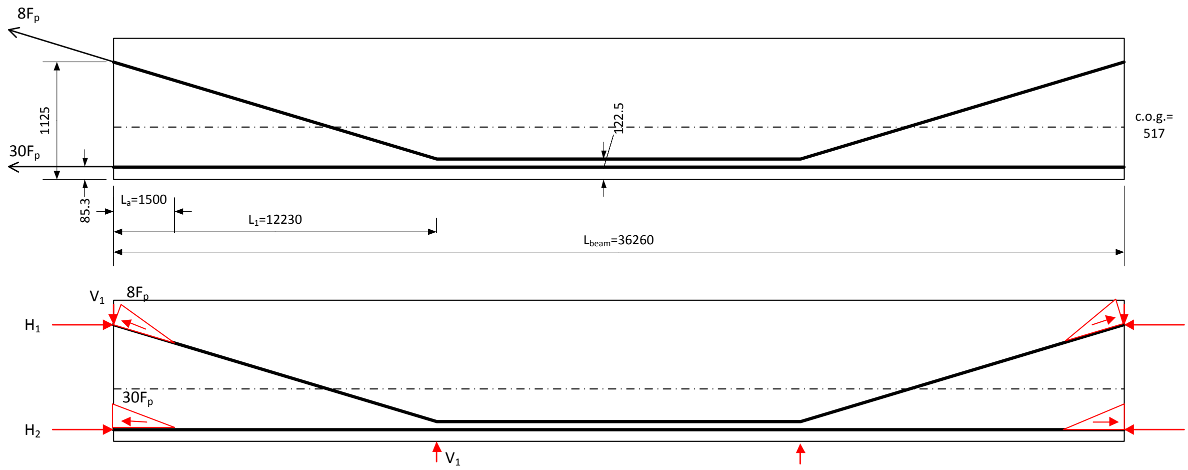

$$H_1 = \frac{L_{devpoint}}{l} \cdot 8 \cdot F_p$$
$$V_1 = \frac{e_4}{l} \cdot 8 \cdot F_p$$
$$H_2 = 30 \cdot F_p$$

Moment, shear and normal force

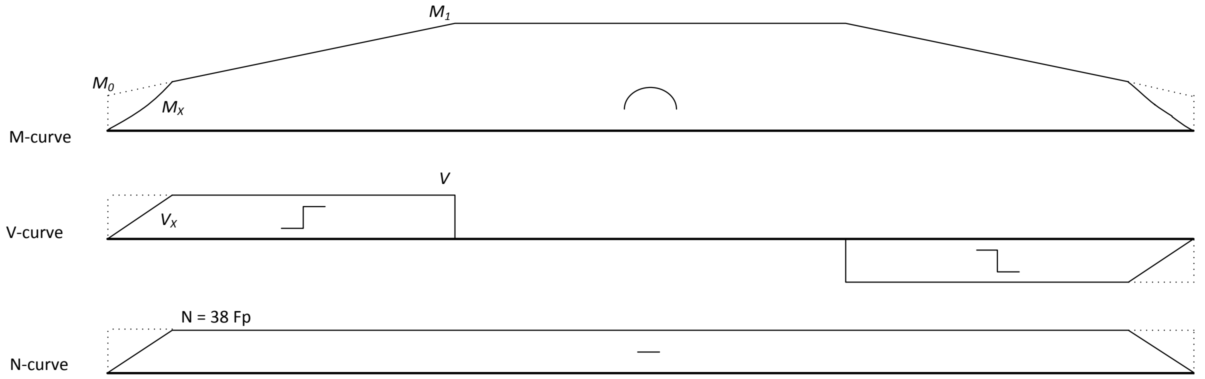

Following a simple method neglecting the bond influence gives enveloping curves:

$$V = V_1$$
$$N = -(H_1 + H_2)$$

$$M_0 = H_1 \cdot e_1 - H_2 \cdot e_2$$
$$M_1 = H_1 \cdot e_1 - H_2 \cdot e_2 - V_1 \cdot L_{devpoint}$$

$$\begin{cases} M(x) = M_0 + \dfrac{x}{L_{devpoint}} \cdot (M_1 - M_0) \text{ for } 0 < \mathrm{x} < \mathrm{L}_{\mathrm{devpoint}} \\ M(x) = M_1 \text{ for } \mathrm{L}_{\mathrm{devpoint}} < \mathrm{x} < \dfrac{\mathrm{L}}{2} \end{cases}$$

Influence of bond length on distributions

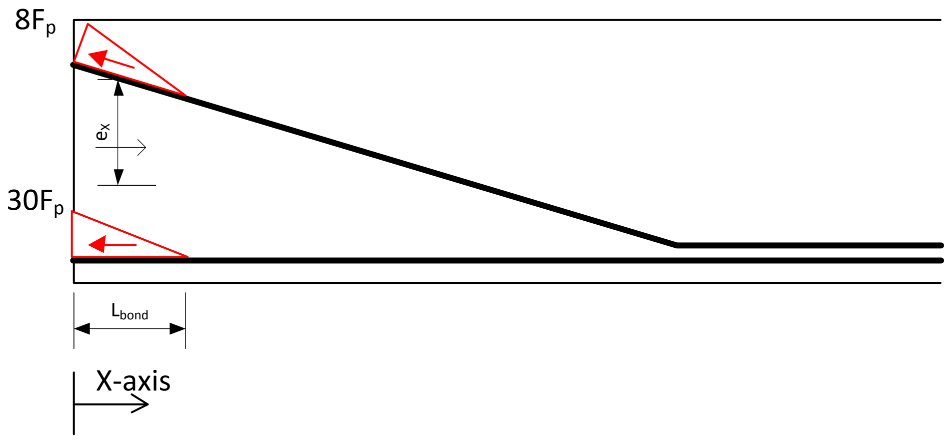

The bond length influences the moment en shear force distribution. Forces and eccentricities are written as functions of X to get the distribution. There is made an distinction between the deviated and straight strands.

$$F_{deviated}(x) = 8 \cdot F_p - \frac{8 \cdot F_p}{L_{bond}} \cdot x$$
$$F_{straight}(x) = 30 \cdot F_p - \frac{30 \cdot F_p}{L_{bond}} \cdot x$$

$$N_{deviated}(x) = \frac{L_{devpoint}}{l} \cdot F_{deviated}(x) = \frac{L_{devpoint}}{l} \cdot \left(8 \cdot F_p - \frac{8 \cdot F_p}{L_{bond}} \cdot x\right)$$
$$N_{straight} = F_{straight} = 30 \cdot F_p - \frac{30 \cdot F_p}{L_{bond}} \cdot x$$

$$V(x) = \frac{e_4}{l} \cdot F_{deviated}(x) = \frac{e_4}{l} \cdot \left(8 \cdot F_p - \frac{8 \cdot F_p}{L_{bond}} \cdot x\right)$$

Difference in the distribution of forces for the bond length.:

$$\Delta N(x) = N_{deviated}(x) + N_{straight} = \frac{L_{devpoint}}{l} \cdot \left(8 \cdot F_p - \frac{8 \cdot F_p}{L_{bond}} \cdot x\right) + 30 \cdot F_p - \frac{30 \cdot F_p}{L_{bond}} \cdot x$$

$$\Delta M(x) = -N_{deviated}(x) \cdot e(x) + N_{straight} \cdot e_2$$
$$= -\frac{L_{devpoint}}{l} \cdot \left(8 \cdot F_p - \frac{8 \cdot F_p}{L_{bond}} \cdot x\right) \cdot \left(e_1 - \frac{e_1 - e_3}{L_{bond}} \cdot x\right) + \left(30 \cdot F_p - \frac{30 \cdot F_p}{L_{bond}} \cdot x\right) \cdot e_2$$

$$\Delta V(x) = -V(x) = -\frac{e_4}{l} \cdot \left(8 \cdot F_p - \frac{8 \cdot F_p}{L_{bond}} \cdot x\right)$$

Resulting force distribution:

$$\begin{cases} \Sigma M(x) = M(x) + \Delta M(x) \text{ for } 0 < \mathrm{x} < \mathrm{L_{bond}} \\ \Sigma M(x) = M(x) \text{ for } \mathrm{L_{bond}} < \mathrm{x} < \frac{\mathrm{L}}{2} \end{cases}$$

$$\begin{cases} \Sigma N(x) = N + \Delta N(x) \text{ for } 0 < \mathrm{x} < \mathrm{L_{bond}} \\ \Sigma N(x) = N \text{ for } \mathrm{L_{bond}} < \mathrm{x} < \frac{\mathrm{L}}{2} \end{cases}$$

$$\begin{cases} \Sigma V(x) = V + \Delta V(x) \text{ for } 0 < \mathrm{x} < \mathrm{L_{bond}} \\ \Sigma V(x) = V \text{ for } \mathrm{L_{bond}} < \mathrm{x} < \frac{\mathrm{L}}{2} \end{cases}$$

E. Detailed information about used FEM

Before modelling some important things are prepared and presented in Part I of the report:

- Calculation of straight bridge (Appendix I-A – Calculation straight bridge)
- Calculation of skew bridge (Appendix I-B – Calculation skew bridge)
- Drawing with all dimensions and details (Appendix I-C – Drawings reinforcement and cables)

Assumptions and simplifications:

- Influences of temperature, creep and shrinkage are neglected. Shrinkage will have some effect, but that shall be very small. Creep is not relevant for the short term traffic loads.
- For the calculation of the reinforcement the method of the VBC, still valid and used by Spanbeton, was used. With this method a design was made as starting point for the model.
- For the model Eurocode is used. Used codes:
    - NEN-EN 1992-1-1 2005 nl, Design and calculation of concrete construction, general rules and rules for buildings.
    - NEN-EN 1992-1-1 NB 2007 nl. National Annex
    - prEN 10138-3,

The program ATENA 3D is chosen to use for this model. This models shall be refined dependent on the considered phenomenon.

Optimization cross-sections

ZIP-girder

Minalu already built a 3D model, linear-elastic, for the skew bridge to compare the results with results of other linear elastic models. In this model the shape shown in Figure E-1 was used.

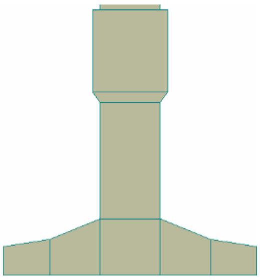

Figure E-1 Equivalent cross-section ZIP used by Minalu

Comparison of the properties of this simplified cross-section with the real ZIP cross-section shows that the simplification is unsafe. Especially the stiffness I_z shows a big deviation.

	ZIP	Simplification	Deviation
A	**5,68E-01**	**5,73E-01**	0,9%
Iy	**1,02E-01**	**1,02E-01**	0,0%
Iz	**2,41E-02**	**2,59E-02**	6,9%
It	**1,39E-02**	**1,40E-02**	0,7%
c ZLCS	**519**	**512**	-1,4%

Table E-1 Comparison cross-section (Figure E-1) with ZIP cross-section

It's important to have an equivalent cross-section that is as accurate as possible. The cross section of Minalu takes a massive bottom part of the cross-section. That part is adapted (Figure E-2), and from the comparison (Table E-2) follows that the new simplification of the cross-section is indeed more accurate. The complexity does not increase because only two nodes are shifted and no elements are added.

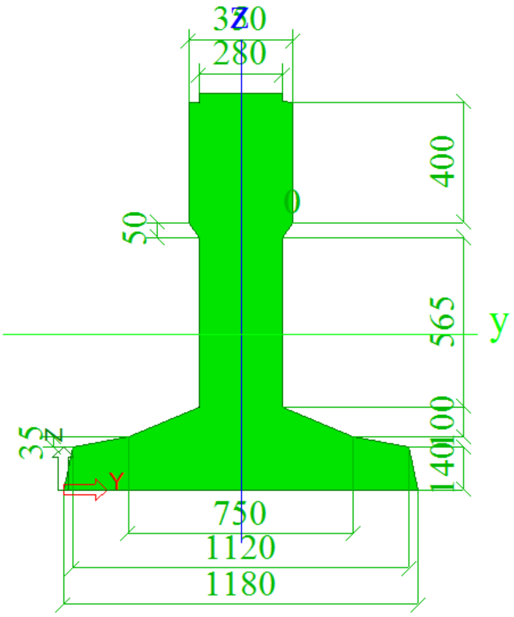

Figure E-2 Equivalent cross-section ZIP non-linear part, simplification 1

	Real ZIP	**Simplification**	Deviation
A	5,68E-01	**5,67E-01**	-0,2%
Iy	1,02E-01	**1,01E-01**	-1,0%
Iz	2,41E-02	**2,40E-02**	-0,4%
It	1,39E-02	**1,40E-02**	0,7%
c ZLCS	519	**517**	-0,4%

Table E-2 Comparison cross-section (Figure E-2) with ZIP cross-section

Check of deformations ZIP-girder

For the ZIP-girder some models are investigated to find a good balance between calculation time and accuracy. Especially the deformations are important because that's the output which is needed.

Applied test load:	10 kN/m -> $3{,}571\cdot10^{-2}$ kN/m^2 on top of girder (width 280 mm)
Length between supports:	35,3 m
Moment of inertia:	$1{,}0175\cdot10^{-1}$ m^4
Distance to top fibre:	0,802 m
Distance to bottom fibre:	0,518 m
Moment:	$1/8\cdot10\cdot35{,}3^2 = 1557.61$ kNm
Stress top:	7,93 N/mm^2
Stress bottom:	12,28 N/mm^2
Deformation:	52,30 mm

Three models are considered;

1. Linear elements, coarse (identical to model of Minalu), 939 elements
2. Quadratic elements, coarse, 939 elements
3. Linear elements, fine, >3000 elements

A comparison is presented in Table E-3.

Model	Stress top [N/mm^2]	Stress bottom [N/mm^2]	Deformation [mm]
Hand calculation	7,93	12,28	52,30
Lin. El. Coarse	6,74	11,31	49,44
Quadr. El. Coarse	9,86	13,99	52,99
Lin. El. Fine	7,16	12,05	52,02

Table E-3 Comparison different models

Obviously model 3 is the best option because it don’t underestimate the deformations, but the calculation time will be much longer than for model 1. Model 2 overestimates the deformation a bit, but also in that case much more calculation time is needed. Model 1 is chosen to be used. The margin of the solution will be investigated, so in later stage it will be visible if this assumption gives troubles.

Material model Large linear-elastic model

In first instance the average values will be used following from the Eurocode. For the values about energy etc. the values given by ATENA will be hold. In practice this are the buttons to fit the model to the test results, in this case there are no tests.

Model girders

The material ‘3D Elastic Isotropic’ is chosen. The title of the material is ‘concrete girders linear elastic’. The properties presented in Table E-4 are used to model the structure. Concrete quality C53/65 is used.

Tab	Constant	Value	Unit
Basic	E	38000	MPa
	ν	0.2	-
Miscellaneous	ρ	$2.5 \cdot 10^{-2}$	MN/m^3
	α	n.v.t.	1/K

Table E-4 Parameters for linear elastic concrete girders

Model deck

The material ‘3D Elastic Isotropic’ is chosen. The title of the material is ‘concrete deck linear elastic’. The properties presented in Table E-5 are used to model the structure. Concrete quality C28/35 is used.

Tab	Constant	Value	Unit
Basic	E	16000 (0.5*32000)	MPa
	ν	0.2	-
Miscellaneous	ρ	$2.5 \cdot 10^{-2}$	MN/m^3
	α	n.v.t.	1/K

Table E-5 Parameters for linear elastic concrete deck

Material model Physical non-linear detail model

For non-linear behaviour the following points are included:

- Reinforcement
- Properties of prestressing cables, including bond model
- Properties of concrete (both girders and deck)

The presented mean strengths are measured from data of Spanbeton. That values are not used in the report.

Properties of reinforcement steel

For the reinforcement the material ‘reinforcement’ is chosen, with properties given in Table E-6 and Figure E-3. The title of the material is ‘reinforcement’. The material B500B of the Eurocode is used.

Tab	**Constant**	**Value**			**Unit**
		Mean	**Characteristic**	**Design**	
Basic	Type	Bilinear (with hardening)			
	E	$2.74 \cdot 10^5$	$2{,}00 \cdot 10^5$		MPa
	σ_y	548.2	500	500/1.15=435	MPa
	σ_t	628.6	500	500/1.15=435	
	ε_{lim}	7.86	n.v.t.		%
	Active in compr.	No			-
Miscellaneous	P	n.v.t.			MN/m^3
	A	n.v.t.			1/K

Table E-6 Parameters for non-linear reinforcement model

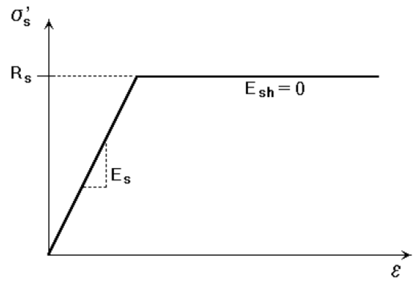

Figure E-3 Bi-linear reinforcement model of ATENA 3D

Properties of prestressing steel

For the prestressing steel also material ‘reinforcement’ is added. The title given to the material is ‘prestressing’. The material Y1860S7 of the EN 10138-3 is used.

The properties as given in Figure E-4 are modelled with the strain hardening. The used values are given in Table E-7.

Tab	**Constant**	**Value**			**Unit**
		Mean	**Characteristic**	**Design**	
Basic	Type	Bilinear with hardening			
	E	$2{,}0 \cdot 10^5$	$1{,}95 \cdot 10^5$		MPa
	σ_y	1737	$0.9 \cdot 1860$ =1674	1674/1.1=1521	MPa
	σ_t	1937	1860	1860/1.1=1690	
	ε_{lim}	6.0	$1.0 \cdot 3.5$		%
	Active in compr.	No			-

Miscellaneous	P	n.v.t.	MN/m^3
	A	n.v.t.	1/K

Table E-7 Parameters for prestressing steel model

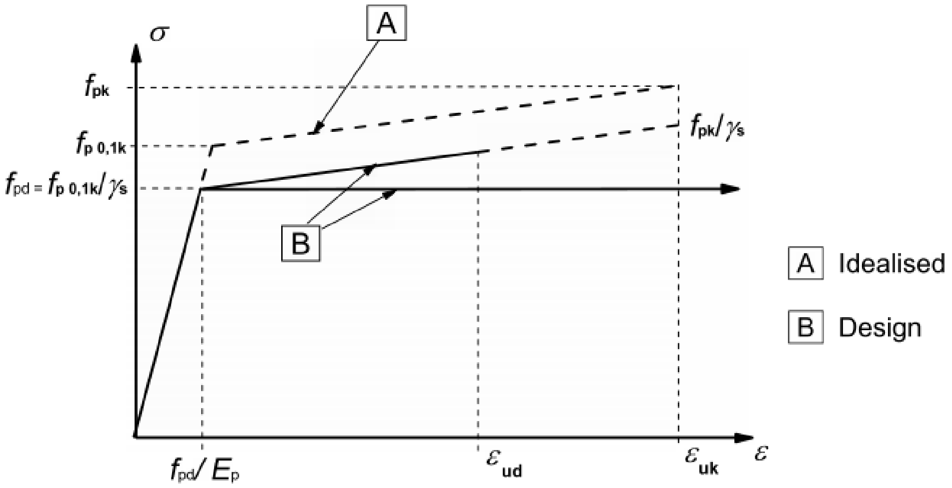

Figure E-4 Properties of prestressing steel according to the Eurocode

A bond model is used to avoid cracking of the girder in the zone where the prestressing force is transferred to the concrete. In ATENA the bond-slip law of Bigaj is available, presented in Figure E-5. The curve depends on two variables, the concrete cubic compressive strength and the bar radius of the reinforcement.

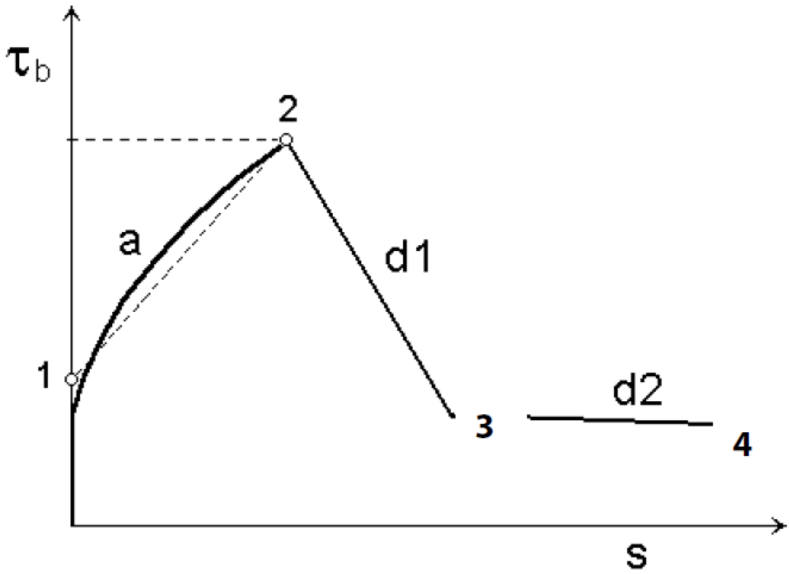

Figure E-5 Bond law by Bigaj 1999

Point	Slip [m]	Bond stress [MPa]
1	0	2.646
2	$5.520 \cdot 10^{-4}$	5.292
3	$6.486 \cdot 10^{-4}$	3.704
4	$6.624 \cdot 10^{-3}$	0

Table E-8 Applied parameters for Bigaj model

Properties of concrete
The philosophy of ATENA is to use a uniaxial stress-strain law to model the 3D effects properly, Figure E-6. The numbers in that figure indicates the state of damage in the structure which can be get from the output of ATENA. The peak values of stress in compression and in tension comes from the biaxial stress state as shown in Figure E-7.

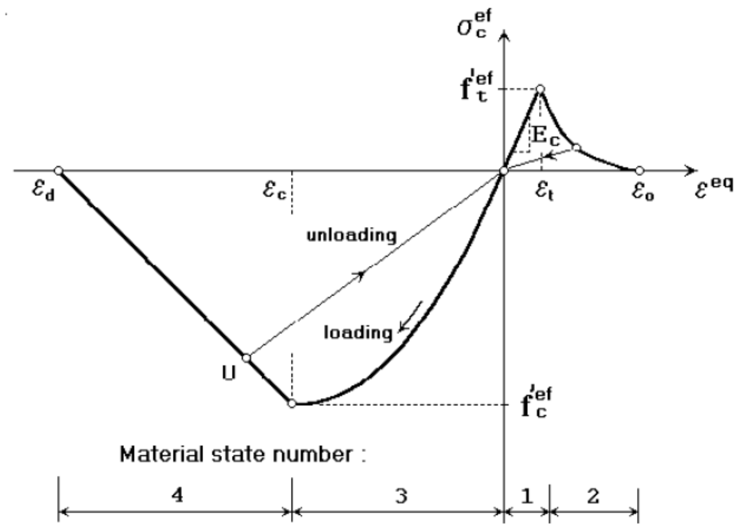

Figure E-6 Uniaxial stress-strain law for concrete of ATENA 3D

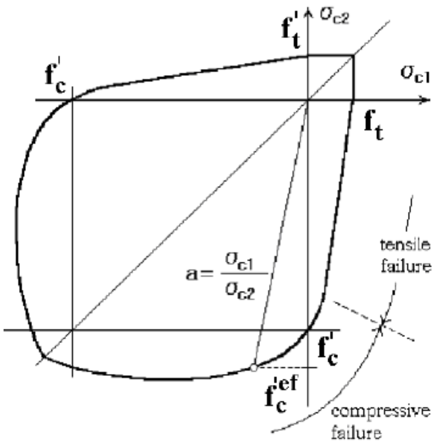

Figure E-7 Biaxial failure function for concrete

The four material states are briefly commented:

1. Tension before cracking: assumed linear elastic.

2. Tension after cracking: fictitious crack model based on crack-opening law and fracture energy. The exponential crack opening law of Hordijk is used, Figure E-8.

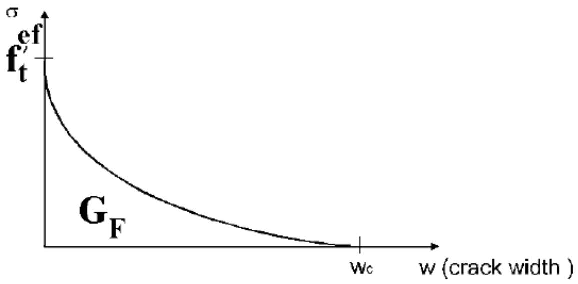

Figure E-8 Exponential crack opening law of Hordijk

3. Compression before peak stress: Formula recommended by CEB-FIP Model Code. Distributed damage is considered before the peak stress is reached, Figure E-9.

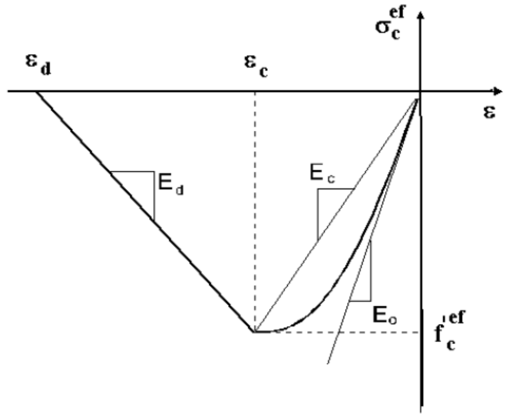

Figure E-9 Stress-strain relation of ATENA for concrete in compression

4. Compression after peak stress: It is assumed that compression failure is localized in a plane normal to the direction of the compressive principal stress. It is assumed that the plastic deformation (w_d) is independent of the size of the structure, Figure E-10. This must be transformed to the stress-strain relation for the corresponding volume of continuous material, as shown in Figure E-9 Stress-strain relation of ATENA for concrete in compressionFigure E-9.

1.

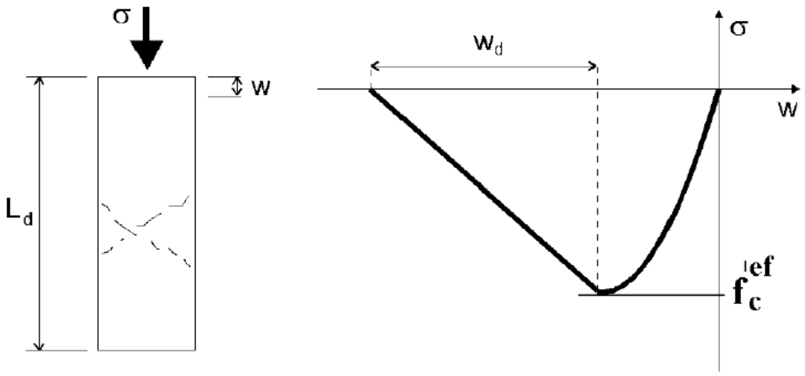

Figure E-10 Compression strength after peak stress

In ATENA 3D the tension cracking behaviour and plastic compression behaviour are combined in a material model called ‘3D Nonlinear Cementitious 2’.

Note: When the crack spacing calculated by the standard algorithm of ATENA is smaller than the element size the calculated widths may be overestimated. In that case the crack width must be reduced manually, ATENA takes the lowest value.

Model girders
The material ‘3D Nonlinear Cementitious 2’ is chosen. The properties presented in Table E-9 are used to model the structure. Concrete quality 53/65 is used.

Tab	Constant	Value			Unit
		Mean	Characteristic	Design	
	f_{cu}		65	65/1.5=43.3	MPa
Basic	E	22*(82.6/10)^0.3 = 41450	38000		MPa
	N	0.2			-
	f_t	2,12*ln(1+82,6/10) = 4,72	2.91	2.91/1.5=1.94	MPa
	f_c	82,6	53	53/1.5=35.3	MPa
Tensile	G_F ($0.000025 \cdot f_t$)	Automatic by ATENA			-
Compres.	W_d	Automatic by ATENA			m
	ε_{cp}	Automatic by ATENA			-
	$r_{c,lim}$	Automatic by ATENA			-
Shear	S_F	Automatic by ATENA			-
	Aggr. Interlock	Automatic by ATENA			
Miscel.us	Fail. surf. excentr.	Automatic by ATENA			-
	B	Automatic by ATENA			-
	P	$2.5 \cdot 10^{-2}$			MN/m^3
	A	n.v.t.			1/K
	Fixed cr. m. coëff.	0			-

Table E-9 Parameters for non-linear concrete girders

F. Simple method to take results from ATENA

Introduction

For one element the process of finding the results is illustrated. For other element types it is assumed that the same procedure is valid.

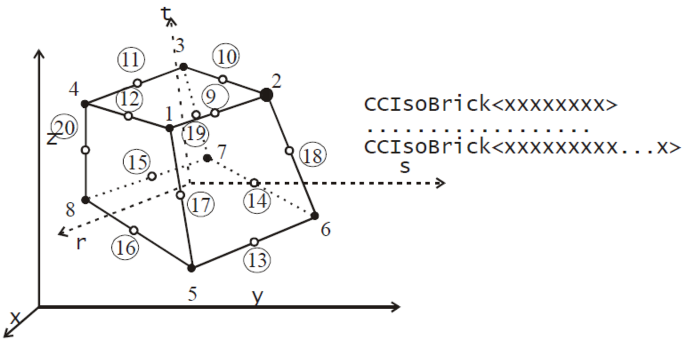

Fig. 3-8 Geometry of CCIsoBrick<...> elements.

(from ATENA 3D theory manual)

Step 1: Macroelements, Geometry of structure

The geometry of the structure is defined with macro-elements. The dimensions are input of the user and thus known. In the output the name for the macroelement is: <u>group</u>

Step 2: Definition of elements, Finite Element Mesh

The mesh is chosen as explained in the manuals of ATENA. The elements are defined by nodes and element numbers. The name for the finite element is: <u>element</u>

The results can be found by clicking  in the Post-processor. You can get the values as follows:

- Nodal coordinates: Step 1 (or other step) -> Nodes -> <u>Reference</u> Nodal Coordinates
- Element indices: Step 1 (or other step) -> Elements -> Element Indices

Nodes

For the nodal coordinates results are given in the following form. There is given an table for every macro-element.

Node	x(1) [m]	x(2) [m]	x(3) [m]
1	value	value	value
2	value	value	value
3	value	value	value
:	:	:	:
N	value	value	value

Example: When there is a macroelement with 4 quadratic finite elements inside that will give 56 nodes in the table.

Elements

The elements are defined by the nodes, the place of the nodes in the element are important. In this way information is connected and the place of the elements is fixed. Following the quadratic brick element as presented above the elements has 20 nodes. This numbers are connected with the node numbers in the following way (example):

Group	Element	No 1	No 2	No 3	No 4	No 5	..	No 6
1	1	3	8	5	n-1	n-10		2

Step 3: Position of Integration Points
When the position of the elements is known the position of the Integration points can be found simply.

Again: The results can be found by clicking  in the Post-processor. You can get the values as follows:

- Integration points: Step 1 (or other step) -> Integration points -> Reference Ip Coordinates

The results are presented as follows (example):

Group	Element	Ipt	x(1) [m]	x(2) [m]	x(3) [m]
1	2	1	value	value	value
1	2	2	value	value	value
1	2	3	value	value	value
:	:	:	:	:	:
1	n	N	value	value	value

Practical

The following steps are practical to obtain solutions from the nodal coordinates:

- Copy-paste the list of reference nodal coordinates in an excel sheet (see remark how to do this).
- Past the results you like to analyse beside this coordinates.
- Use 'sorting and filtering' (see illustrations) and use the filter to select a point from the (enormous!!) long list.

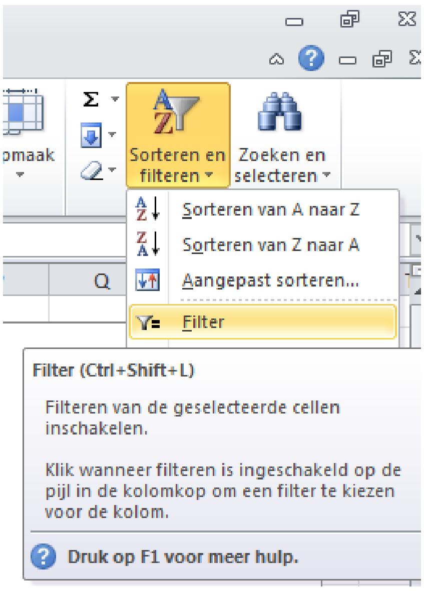

	A	B	C	D	E	F	G	H	I	J	K	L
1	COÖRDINATEN					SPANNINGEN						
2		X	Y	Z								
3							SIGMA XX	SIGMA YY	SIGMA ZZ	TAU XY	TAU YZ	TAU XZ
4												
5	ANALYSIS STEP 5					ANALYSIS STEP 5						
6	POSITION: NODES					POSITION: NODES						
7	MACROELEMENT 1 - REFERENCE NODAL COORDINATES					MACROELEMENT 1 - STRESS						
8	Reference nodal coordinates					Stress						
9	Node	x(1) [m]	x(2) [m]	x(3) [m]		Node	Sigma xx [MPa]	Sigma yy [MPa]	Sigma zz [MPa]	Tau xy [MPa]	Tau yz [MPa]	Tau xz [MPa]
10	1	-2,00E-01	0,00E+00	2,00E-01		1	-9,15E-01	-1,93E-01	-6,90E+00	1,21E+00	7,22E+00	-2,24E+00
11	2	2,00E-01	0,00E+00	2,00E-01		2	-2,46E+01	-4,80E+01	-3,40E+01	-1,53E+00	3,96E+00	4,49E+00
12	3	2,00E-01	0,00E+00	5,00E-01		3	9,14E-01	-3,34E+00	-3,51E+00	-1,81E+00	-8,01E+00	1,58E+00
13	4	-2,00E-01	0,00E+00	5,00E-01		4	3,18E+01	7,97E+01	2,85E+01	-6,55E-02	-7,00E+00	-1,74E-01
14	5	0,00E+00	-4,00E-02	3,50E-01		5	-2,28E+01	-5,03E+01	-2,75E+01	1,41E+00	2,25E+00	1,24E+00
15	6	1,00E-01	-2,00E-02	2,75E-01		6	-1,16E+01	-2,11E+01	-1,93E+01	-1,52E+00	2,21E+00	2,86E+00
16	7	-1,00E-01	-2,00E-02	2,75E-01		7	-1,19E+01	-2,52E+01	-1,72E+01	1,31E+00	4,73E+00	-5,02E-01
17	8	0,00E+00	0,00E+00	2,00E-01		8	-1,07E+01	-2,09E+01	-1,78E+01	-3,62E-01	4,77E+00	7,00E-01
18	9	2,00E-01	0,00E+00	3,50E-01		9	3,15E+00	1,11E+01	-4,16E+00	-3,81E+00	-3,24E+00	3,47E+00
19	10	1,00E-01	-2,00E-02	4,25E-01		10	-4,65E+00	-1,15E+01	-9,47E+00	-3,62E-01	-3,06E+00	1,30E+00
20	11	-1,00E-01	-2,00E-02	4,25E-01		11	1,53E-01	2,52E+00	-3,20E+00	9,94E-01	-3,31E+00	-4,58E-03
21	12	0,00E+00	0,00E+00	5,00E-01		12	1,36E+00	1,38E+00	-2,07E+00	1,20E+00	-6,29E+00	2,69E-01
22	13	-2,00E-01	0,00E+00	3,50E-01		13	1,34E+01	3,66E+01	8,14E+00	7,71E-01	9,34E-01	-7,83E-01
23	14	0,00E+00	0,00E+00	3,50E-01		14	-5,19E-04	-1,77E+00	-5,20E+00	-3,04E-01	-3,97E-01	-3,30E-01

For the integration points the same procedure can be used. Only the values aren't nice values, you can use another filter to search for coordinates between two boundaries.

Remarks:

1. The results can be exported to excel by control + A, then control + C and paste it than in an excel-sheet.
2. In my case X(1), X(2) and X(3) corresponds with X, Y and Z. But you have to verify that!

G. Maple sheet to determine torsional moments from rotations

> $restart; It := 1.39e-2 : G := 15.833e6 : E := 38e6 : Cw := 100e-5 :$
> $G \cdot It; E \cdot Cw;$

$\mathrm{phi} := -2.627e-11 \cdot x^6 + 2.299e-9 \cdot x^5 - 7.863e-8 \cdot x^4 + 1.237e-6 \cdot x^3 - 1.567e-6 \cdot x^2 + 2.788e-5 \cdot x - 3.080e-3;$

$dY := diff(\mathrm{phi}, x) : ddY := diff(dY, x) : dddY := diff(ddY, x) :$
$Mtwringing := G \cdot It \cdot dY :$
$Mtwelving := -E \cdot Cw \cdot ddY :$
$Mt := Mtwringing + Mtwelving;$
$with(plots) :$
$a := plot(Mtwringing, x = 0.63 ..35.63, color = \text{"NavyBlue"}); b := plot(Mtwelving, x = 0.63 ..35.63, color = \text{"Green"}); c := plot(Mt, x = 0.63 ..35.63, color = \text{"Red"})$

> $display(a, b, c, title = \text{"wringing"});$